Journal of Medicinal Chemistry

Article

Development, Optimization and Structure–Activity Relationships of Covalent-Reversible JAK3 Inhibitors Based on a Tricyclic Imidazo[5,4-d]pyrrolo[2,3-b]pyridine Scaffold.

Michael Forster, Apirat Chaikuad, Teodor Dimitrov, Eva Döring, Julia Holstein, Benedict-Tilman Berger, Matthias Gehringer, Kamran Ghoreschi, Susanne Müller, Stefan Knapp, and Stefan A. Laufer

J. Med. Chem., **Just Accepted Manuscript** • DOI: 10.1021/acs.jmedchem.8b00571 • Publication Date (Web): 31 May 2018

Development, Optimization and Structure–Activity Relationships of Covalent-Reversible JAK3 Inhibitors Based on a Tricyclic Imidazo[5,4-d]pyrrolo[2,3-b]pyridine Scaffold.

*Michael Forster[†], Apirat Chaikuad[§,&], Teodor Dimitrov[†], Eva Döring[†], Julia Holstein[#], Benedict-Tilman Berger[§,&], Matthias Gehringer[†], Kamran Ghoreschi[#], Susanne Müller[&], Stefan Knapp[§,&,%], Stefan A. Laufer[†]**

[†]Department of Pharmaceutical / Medicinal Chemistry, Eberhard Karls University Tübingen, Auf der Morgenstelle 8, 72076 Tübingen, DE

[&]Institute for Pharmaceutical Chemistry, Johann Wolfgang Goethe University, Max-von-Laue-Str. 9, D-60438 Frankfurt am Main, DE

[§]Structure Genomics Consortium, Johann Wolfgang Goethe University, Buchmann Institute for Molecular Life Sciences, Max-von-Laue-Str. 15, D-60438 Frankfurt am Main, DE

[#]Department of Dermatology, University Medical Center, Eberhard Karls University Tübingen, Liebermeisterstr. 25, 72076 Tübingen, DE

[%]German Cancer Consortium, DKTK, Site Frankfurt/Mainz, DE

KEYWORDS: Janus kinases, kinome selectivity, covalent-reversible inhibitor, inflammation

ABSTRACT. Janus kinases are major drivers of immune signaling and have been the focus of anti-inflammatory drug discovery for more than a decade. Because of the invariable co-localization of JAK1 and JAK3 at cytokine receptors, the question if selective JAK3 inhibition is sufficient to effectively block downstream signaling has been highly controversial. Recently, we discovered the covalent-reversible JAK3 inhibitor FM-381 (**23**) featuring high isoform and kinome selectivity. Crystallography revealed that this inhibitor induces an unprecedented binding pocket by interactions of a nitrile substituent with arginine residues in JAK3. Herein we describe detailed structure activity relationships necessary for induction of the arginine pocket and the impact of this structural change on potency, isoform selectivity and efficacy in cellular models. Furthermore, we evaluated the stability of this novel inhibitor class in *in vitro* metabolic assays and were able to demonstrate an adequate stability of key compound **23** for *in vivo* use.

INTRODUCTION. The four Janus kinases JAK1, JAK2, JAK3 and TYK2 form a small subfamily of cytosolic tyrosine kinases with pivotal importance for the signal transduction of interleukins (ILs), interferons (IFNs) and other cytokines.[1] As non-receptor tyrosine kinases, JAKs bind to the activated cytokine receptors transmitting extracellular signals by phosphorylation of signal transducers and activator of transcription (STAT) proteins. The phosphorylated STAT proteins dimerize, translocate to the nucleus and act as transcription factors affecting many cellular functions.[2] Although each JAK fulfills important functions in hematological and immunological pathways, the JAK3 isoform features some unique properties compared to the other family members. While JAK1, JAK2 and TYK2 are found in many different cell types and tissues, the expression of JAK3 is mainly restricted to leukocytes having

a key role in the development and maturation of T-cells, B-cells and natural killer (NK) cells.[3] Therefore, JAK3 knock-out or loss-of-function mutations in the kinase- or receptor-genes result in the phenotype of severe combined immunodeficiency (SCID), a general immunological disorder characterized by a complete absence of T- and NK-cells. Besides these serious consequences in the immune system, SCID patients are not affected by other defects highlighting the isolated role of JAK3 in immune signaling.[4-5] This suggests that JAK3-selective inhibition may be a valuable therapeutic strategy to achieve immunosuppression with less adverse effects compared to known immunosuppressive panJAK inhibitors.[6-7] However, none of the disease causing JAK3 mutations are localized to the catalytic domain and the invariant co-localization of JAK3 with JAK1 suggests that inhibition of JAK3 catalytic activity may not be sufficient for full inhibition of this signaling pathway.[8] In recent years it has been therefore fiercely discussed among medicinal chemists whether specific inhibition of JAK3 catalytic activity would be sufficient to achieve immunosuppression or if concomitant inhibition of JAK1 is required to abrogate cytokine signaling.[9-11] Mouse models largely confirmed the SCID phenotype, but catalytically inactive JAK3 variants that could shed light on the scaffolding role of JAK3 in the activated receptor-kinase complexes have not been generated in mice so far. To validate the usefulness of selective inhibition, much effort has been undertaken in the last decade by industry as well as academia to develop isoform specific inhibitors[12-13] and a number of inhibitors with different selectivities within the JAK family are under clinical investigation.[14] Currently, the most prevalent inhibitors for interrogating JAK dependent signaling are baricitinib and tofacitinib (**1**, Figure 1), which are both approved as second-line treatment for rheumatoid arthritis.[15] Contrary to initial reports claiming it to be JAK3 specific, **1** is a panJAK inhibitor making it unsuitable to address the JAK1 vs. JAK3 signaling issue.[10] Another prominent JAK3

inhibitor is NIBR3049 (**2**, Figure 1), which shows a more favorable isoform selectivity profile with a 130 to 1000-fold specificity for JAK3 vs. JAK1, JAK2 and TYK2, respectively. However, this compound potently inhibits several off-targets within the kinome (namely PKCα, PKCθ and GSK3β) in the lower nanomolar range.[16] Due to the high structural similarity of the four JAKs, the design of isoform specific inhibitors is a demanding task. One of the few essential structural differences is a cysteine residue (C909) located in the solvent exposed front part of the ATP binding pocket, which is exclusively found in JAK3. The latter is replaced by a serine in the three other isoforms of the kinase family.[17] The presence of a cysteine in the proximity of the ATP binding site provides the opportunity to achieve selectivity by covalent targeting with electrophilic inhibitors.[18-19] This concept was pursued by many groups in the last years and the highly selective JAK3 inhibitors which originated from these efforts have been recently reviewed.[20-26] In 2016, we reported the discovery of FM-381 (**23**, Figure 1), a covalent-reversible JAK3 inhibitor with an outstanding selectivity within the JAK family and the whole kinome.[27] This compound has been included in the Structural Genomics Consortium's (SGC) Chemical Probe pool[28] and has been rated as a "4-Star-Probe" in the Chemical Probe Portal[29] as a selective tool for the elucidation of JAK3 dependent signaling. In this paper we provide an expanded insight into the structure activity relationships (SARs) and further investigations of physicochemical and metabolic properties of the underlying inhibitor class.

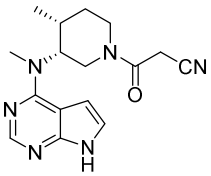

Tofacitinib (**1**)

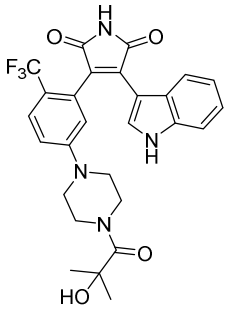

NIBR3049 (**2**)

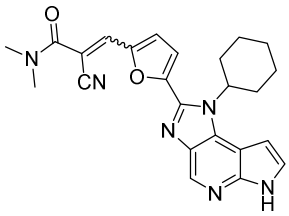

FM-381 (**23**)

Figure 1. Structures of known reference JAK inhibitors discussed in this study.

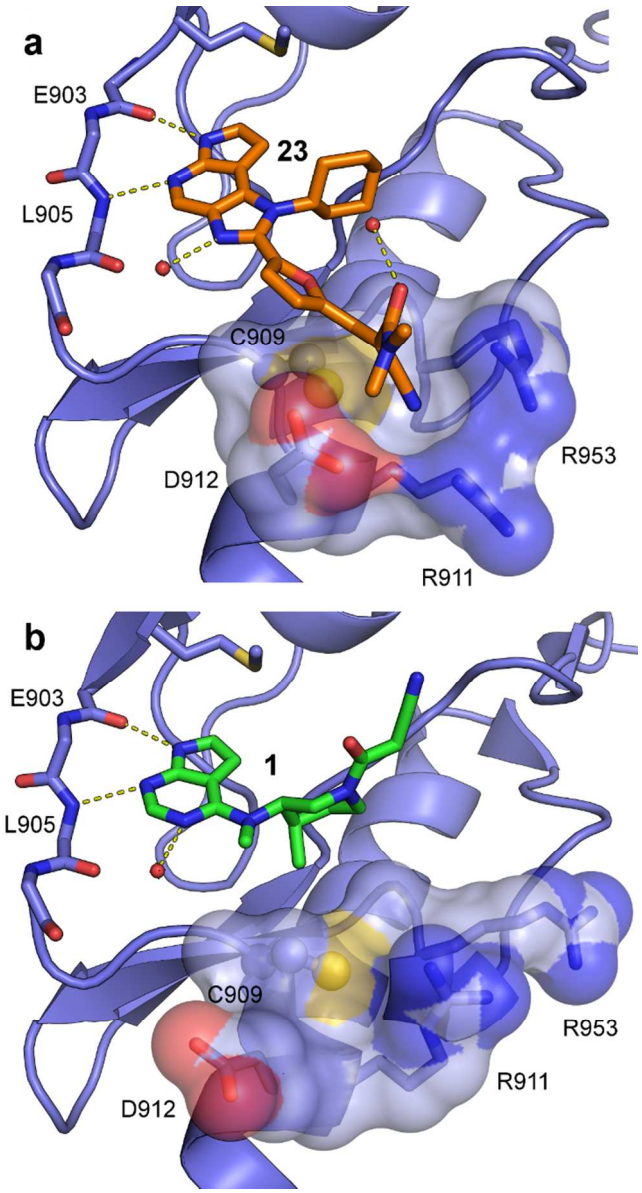

Figure 2. (a) Compound **23** bound to JAK3 (PDB: 5LWM) **(b)** Compound **1** bound to JAK3 (PDB: 3LXK). Comparison of the protein surfaces surrounding C909 (illustrated as ball/stick) shows that **23** induces a distinct binding pocket by interaction of the nitrile substituent and R911. The cavity is generated by significant rearrangement of the sidechains of R911 and R953.

RESULTS AND DISCUSSION. **JAK3 Structure Activity Relationships.** During the analysis of the X-ray structure of JAK3 in complex with compound **23** (PDB: 5LWM) we

discovered a new binding pocket induced by the nitrile substituent of the inibitor's α-cyanoacrylamide warhead (Figure 2a). This cavity is located in close proximity to the covalently targeted C909 and is formed by significant rearrangement of two arginine sidechains (R911 and R953). So far, this induced-fit binding pocket was only observed in the crystal structures of compound **23** and a close analogue (PDB: 5LWN) while it is not present in any other JAK3 structure deposited in the PDB (Figure 2b).[27] To get a more detailed insight into the SARs regarding this "arginine pocket" and to evaluate its impact on potency and selectivity, we iteratively modified the electrophilic warhead of compound **23** by removal of the nitrile or the amide group from the α-cyanoacrylamide motif or by saturation of the α,β-double bond. These structural modifications were applied to different linkers (para-/meta-phenyl and 2,5-furyl) to cover all relevant angles between the hinge-binding motif and the sidechain directed towards R911. The compounds were initially tested in our activity-based in-house ELISA[30] to evaluate JAK3 inhibition on the isolated enzyme (Table 1). In this assay format both reference compounds **1** and **2** demonstrated excellent JAK3 potency in the lower nanomolar range with IC_{50} values of 3.5 nM for **1** and 11 nM for **2**, respectively. The first investigated compound series were acrylamides and their corresponding saturated analogues. For both, the meta- and para-phenyl linkers, the corresponding acrylamide derivatives **3**, **4**, **6** and **7** exhibited only moderate to weak inhibitory activity, ranging from micromolar to triple-digit nanomolar IC_{50} values. However, it is worth mentioning that primary amide **3** precipitated under the assay conditions due to an insufficient aqueous solubility. Saturation of the double bond and therefore inactivation of the Michael system (compounds **12**, **13**, **15** and **16**) gave IC_{50} values in similar range with a maximally 3-fold decrease in activity, which was not substantial enough to assume a covalent targeting of C909 by this inhibitor class. These subtle changes are more probably caused by

entropic effects due to the increased flexibility of the saturated alkyl chain. The replacement of the phenyl linker by a 2,5-disubstituted furan moiety generally resulted in better inhibitory activities. While a similar 3-fold decrease in potency was observed for the saturated dimethylamide analogue **17** (IC_{50} = 181 nM) compared to the parent dimethylacrylamide **8** (IC_{50} = 51 nM), the primary amides **5** and **14** surprisingly showed the reversed trend with IC_{50} values of 129 nM for acrylamide **5** and 59 nM for the saturated derivate **14**. This somewhat better potency of **14** may be explained by the formation of an intramolecular hydrogen bond between the primary amide and the furan oxygen atom. This would result in a reduced flexibility and hydration and therefore having a positive entropic effect and less desolvation penalty.

In a second series the amide function was replaced by a cyano substituent leading to acrylonitriles **9-11** and the corresponding saturated analogues **18-20**. The para-substituted phenyl linker again provided only moderate inhibition levels with IC_{50} values around 400 nM for the unsaturated and saturated derivatives **9** and **18**. In contrast a 4-fold difference in JAK3 inhibition was determined for the corresponding meta-phenyl linked acrylonitrile **10** (IC_{50} = 135 nM) and its saturated analog **19** (IC_{50} = 505 nM). Moreover, **10** exhibited a significantly lower IC_{50} compared to the corresponding amide derivatives **4** and **7** (IC_{50} values of 470 nM and 548 nM, respectively). Again, the furyl linker yielded the most potent JAK3 inhibition within this series with IC_{50} values of 27 nM for acrylonitrile **11** and 129 nM for alkylnitrile **20**. To elucidate the role of the nitrile substituent, X-ray structures were determined for compounds **10**, **11** and **20** in complex with JAK3 (Figure 3). All compounds showed a binding mode similar to **23** (Figure 1a) with two hydrogen bonds formed with the backbone of the hinge residues E903 and L905. The cyclohexyl moiety occupies the region of the ATP binding pocket. The linker is orientated towards the solvent exposed front part of the catalytic cleft, positioning the nitrile substituents in

close proximity to C909, R911 and R953. The alkylnitrile sidechain of **20** showed no directed interactions to these residues (Figure 3c) and the conformation of R911 and R953 was comparable to that seen in the X-ray structure of **1** (Figure 2b). In sharp contrast, both acrylonitriles **10** and **11** induce the formation of the arginine pocket and interact with R911 (Figure 3a,b) in the same way as observed in the crystal structure of **23** (Figure 2a). These structural models together with the assay data demonstrated that both, the furan linker as well as the acrylonitrile substituent and the resulting formation of the arginine pocket, are two distinct factors positively influencing JAK3 inhibitory potency.

Table 1. ELISA-based JAK3 inhibition data

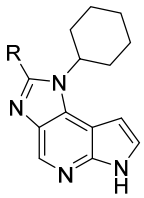

Compd.	R =	JAK3 IC_{50} [nM]	Compd.	R =	JAK3 IC_{50} [nM]
Tofacitinib (**1**)	n.a.	3.5 ± 0.6^{a}	NIBR3049 (**2**)	n.a.	11 ± 1^{b}
Series 1: amide-substituted inhibitors					
3	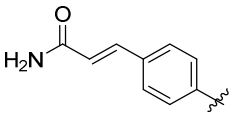	$> 1000^{b,c}$	**12**	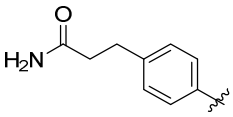	499 ± 48^{b}
4	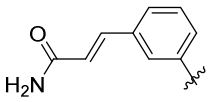	470 ± 36^{b}	**13**	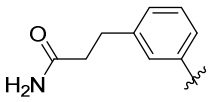	490 ± 9^{b}
5	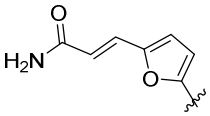	129 ± 8^{b}	**14**	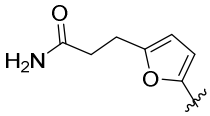	59 ± 2^{b}

6	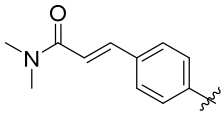	226 ± 31[b]	**15**	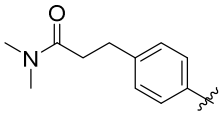	642 ± 63[b]
7	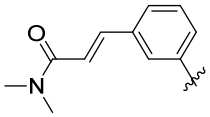	548 ± 39[b]	**16**	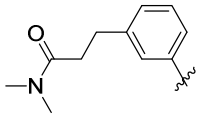	678 ± 25[b]
8	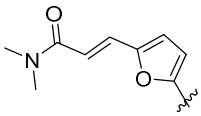	51 ± 6[b]	**17**	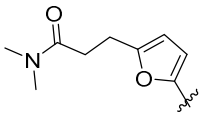	181 ± 14[b]
Series 2: nitrile-substituted inhibitors					
9	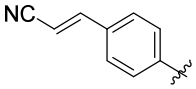	390 ± 156[b]	**18**	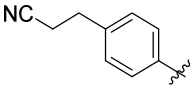	436 ± 15[b]
10	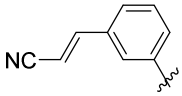	135 ± 3[b]	**19**	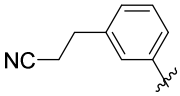	505 ± 41[b]
11	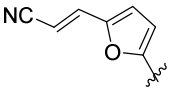	27 ± 1[b]	**20**	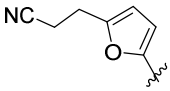	129 ± 13[b]
Series 3: covalent-reversible inhibitors					
21	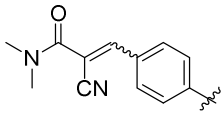	571 ± 24[b]	**25**	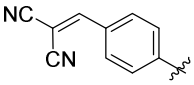	30 ± 6[b,d]
22	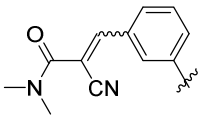	205 ± 8[b]	**26**	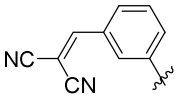	11 ± 1[b,d]
23	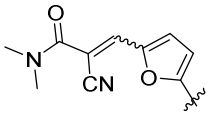	9 ± 1[b]	**27**	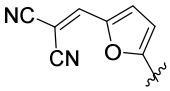	4 ± 1[b,d]
24	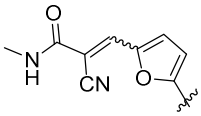	23 ± 3[b]	**28**	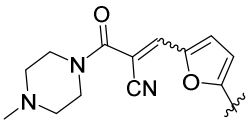	14 ± 2[b]

IC_{50} values are calculated from the results of an ELISA.[30] [a]average ± SD (n = 18) [b]average ± SEM (n = 3) [c]precipitation from aqueous assay buffer [d]arylidene dinitriles show unspecific reactivity with assay buffer components.

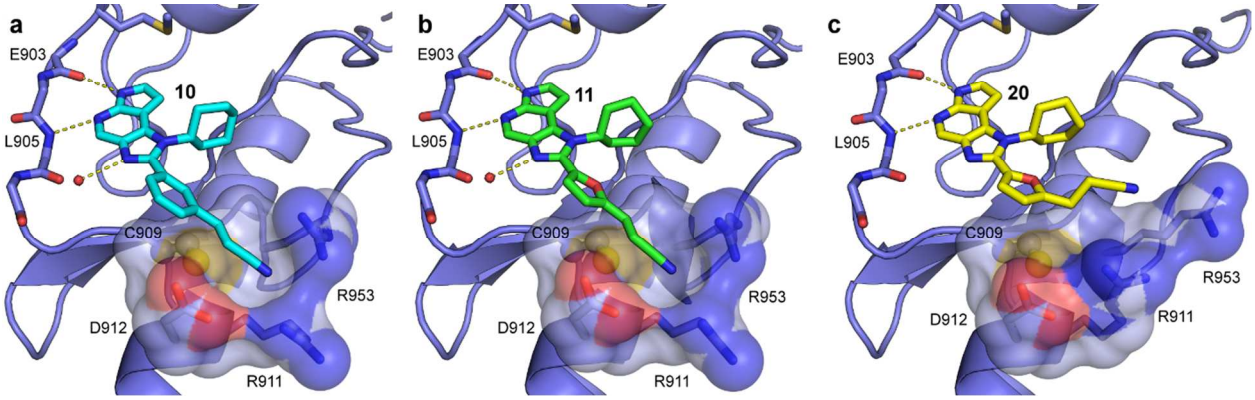

Figure 3. (a) Compound **10** bound to JAK3 (PDB: JAK3-**10**) (b) Compound **11** bound to JAK3 (PDB: JAK3-**11**) (c) Compound **20** bound to JAK3 (PDB: JAK3-**20**). Acrylonitriles **10** and **11** induce the arginine pocket as observed in the JAK3 complex with compound **23**. Saturated alkylnitrile **20** was not able to induce this cavity and R911 and R953 shared similar conformation as observed in the crystal structure of **1**.

In a third series we combined the nitrile and amide substituents resulting in cyanoacrylamides, a compound class, which was previously described as covalent-reversible Michael acceptors.[31] Comparison of inhibitory activities of compounds **21**, **22** and **23** with the corresponding acrylonitriles **9**, **10** and **11** reveals that only the furan linked compound **23** benefits from the additional electron-withdrawing effect of the amide group. While phenyl linked compounds **21** and **22** only show low to moderate JAK3 inhibition (IC_{50} values of 571 nM and 205 nM, respectively), compound **23** exhibits an IC_{50} value of 9 nM, which is close to the lower resolution limit of the applied ELISA. Further modifications of the dimethyl amide of **23**, like truncation of a methyl group (**24**) or replacement by an N-methylpiperazine (**28**), were also well tolerated and resulted in low nanomolar IC_{50} values (23 nM and 14 nM for **24** and **28**, respectively). The observed significant difference in the inhibitory potency of **23** compared to **22** suggested that covalent bond formation with C909 was limited to the furan-linked **23** and not possible with the

phenyl bearing **22**. Although there was no covalent bond observed in the X-ray structure of **23** (Figure 2a), covalent bond formation was observed for a close analogue of **23** by mass spectroscopic and crystallographic data as reported earlier.[27] Moreover, comparison of the X-ray structures of **10**, **11** (Figure 3a,b) and **23** (Figure 2a) revealed significant differences in the dihedral angles along the α,β-double bond of the Michael system. While the usual trans angle of 180° (measured as 179° and 178°) was retained in the structures of **10** and **11**, the double bond of **23** was fairly distorted with a dihedral angle of 149°. This out-of-plane conformation of **23** may be due to interaction with the electrophilic β-carbon atom with the thiol group of C909 leading to bond formation.

We further enhanced the electrophilicity of the Michael acceptor in the compounds **25-27** by replacing the amide function by a second nitrile group. With IC_{50} values in the lower nanomolar range, these benzylidene malononitriles were remarkably potent JAK3 inhibitors and contrary to the corresponding cyanoacrylamides **21-23**, the linker geometry had a significantly lower influence on potency. It should be mentioned that the structural element of arylidene dinitriles is relatively promiscuous and shows a high reactivity towards any nucleophile. Indeed, subsequent chemical incubation experiments revealed an unspecific reactivity for the highly electrophilic inhibitors **25-27** towards thiol nucleophiles. Dithiothreitol (DTT) is a common reductant and an important ingredient of standard kinase assay buffer systems. As an aliphatic thiol, it possesses a nucleophilicity comparable to cysteine and is therefore capable to react in a similar way via Michael addition with electrophilic inhibitors. While no decomposition was observed for inhibitors **25-27** in methanolic solution, the compounds degraded over time in presence of DTT-containing kinase assay buffer. In contrast, cyanoacrylamides showed reversible addition of the thiol without any signs of further decomposition (data not shown). Because of the high and

unspecific reactivity of the arylidene dinitrile moiety the inhibitory activity of **25-27** may not only be attributed exclusively to the interaction with C909 and data obtained with this type of compounds should be interpreted carefully. Nevertheless, compounds from this class showed remarkable JAK3 potency and selectivity even in cells or in the presence of thiol-containing buffer (*vide supra*).

For covalent inhibitors, the binding of the ligand can be divided into two steps: first a reversible binding event and second the formation of the covalent bond between electrophile and the cysteine sidechain.[32] Since the initial reversible inhibitor binding is required before a covalent bond to C909 can be formed, it is important that the inhibitor shows not only a high reactivity towards sulfur nucleophiles, but also successfully competes with the high intracellular ATP concentrations. In order to evaluate the contributions of reversible versus covalent binding to the overall inhibitory potency of compound **23**, we modified our lead compound with the goal of modulating the reversible binding affinity while retaining the electrophilic cyanoacrylamide warhead (Figure 4). The truncation of the cyclohexyl sidechain (compound **29**, Figure 4), which fills the ATP binding pocket towards the glycine rich loop, results in an IC_{50} value of 368 nM, corresponding to a more than 40-fold loss in potency compared to **23**. As expected, an even more drastic drop in potency resulted from the methylation of the pyrrole nitrogen atom (compound **30**, Figure 4). This modification prevents the formation of key hydrogen bonds to the hinge region and caused a complete loss of inhibitory activity towards JAK3 even at concentrations up to the micromolar range. These data demonstrated that the high potency of **23** was not only driven by the covalent interaction with C909, but also originates from strong reversible interactions.

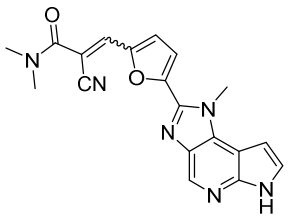

29

JAK3 IC_{50} = 368 ± 41 nM

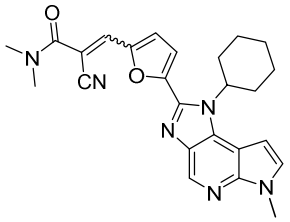

30

JAK3 IC_{50} > 10 000 nM

Figure 4. Structures and inhibition data of compounds **29** and **30**. IC_{50} values are calculated from the results of an ELISA[30] as average ± SEM (n = 3)

Kinase Selectivity Profiles. As a next step in the development process, we determined JAK family selectivity profiles of selected compounds of the furyl series in a radiometric assay format carried out at Reaction Biology Corp. (Table 2). In this more sensitive assay, reference compound **1** showed a subnanomolar JAK3 IC_{50} value of 0.29 nM and, as expected, poor JAK isoform selectivity as reported earlier.[10] While **1** inhibited JAK1, JAK2 and JAK3 with a similar potency, TYK2 was inhibited to a lower extent. Maleimide **2** showed a better JAK3 selectivity, comparable with the previously reported data.[11, 16] Meanwhile acrylamide **8** and its saturated analogue **17** showed significantly higher IC_{50} values compared to reference compounds **1** and **2** and did not exhibit a noteworthy JAK3 selectivity as well. In contrast, a huge difference in selectivity and potency was observed between acrylonitrile **11** and its saturated counterpart **20**. While **20** featured a similar selectivity profile and moderate potency as the amide derivatives **8**

and **17**, compound **11** showed potent JAK3 inhibitory activity equal to **1** (IC_{50} = 0.21 nM) with a 57-, 250- and 210-fold selectivity against JAK1, JAK2 and TYK2, respectively. This remarkable leap in selectivity together with the crystallographic structural information disfavoring covalent binding of **11** and **20** (Figure 3b,c) provides strong evidence that the induction of the arginine pocket may be an additional key driver for JAK3 selectivity. Nevertheless, the excellent selectivity profile was even further improved when a covalent-reversible Michael acceptor was introduced. Compound **23** provided an extraordinarily potent JAK3 inhibition (IC_{50} = 0.13 nM) combined with good isoform selectivity (400-, 2700- and 3600-fold vs. JAK1, JAK2 and TYK2, respectively). As mentioned before we hypothesize that this improved isoform selectivity of **23** compared to **11** can be attributed to a synergism between the formation of the arginine pocket and a covalent-reversible interaction to C909 enabled by the additional electron withdrawing effect of the amide group of **23**.

It is known, that JAK3 has a higher affinity to ATP compared to the other JAK isoforms, which causes a shift in selectivity when the assays are performed at constant and higher ATP concentrations compared to the typically determined data at K_m ATP.[11, 20] To investigate the ATP dependency of the isoform selectivity of **23**, IC_{50} values were determined at an ATP concentration of 200 μM and revealed a retention of the favorable selectivity profile at this physiologically more relevant ATP concentration. This 20-fold higher ATP concentration better reflects the typical intracellular conditions with even higher ATP levels in the low millimolar range. While under these conditions the JAK3 inhibitory potency of **23** remained single digit nanomolar (IC_{50} = 2 nM), an at least 330-fold selectivity window over JAK1 was observed (IC_{50} = 668 nM) and the IC_{50} values for JAK2 and TYK2 even increased up to the micromolar range (Table 2). As reported earlier,[27] this compound was also screened against the activity based

ProQinase panel of 410 kinases and proved to be highly JAK3 selective showing no off-targets at a concentration of 100 nM and only eleven hits with more than 50% inhibition at a higher 500 nM cut-off (Table S2). Moreover, there was no significant inhibition of the other ten human kinases which are carrying a cysteine residue at a position equivalent to JAK3.[19] Derivatization of the amide residue of **23** maintains a good JAK3 selectivity, as shown by compound **28** carrying an N-methylpiperazinyl amide. While **28** shows a slightly weaker inhibition of JAK3 (IC_{50} = 0.74 nM) compared to **23**, it still exhibits a favorable selectivity against the other isoforms with a 160-fold window over JAK1 and an at least 1000-fold selectivity towards JAK2 and TYK2. Despite showing a certain instability in thiol-containing buffer systems as described above, the arylidene dinitrile **27** also exhibits an evident JAK3 selectivity with a subnanomolar IC_{50} of 0.39 nM and a 10- to 470-fold selectivity over the three other isoforms. The moderate isoform selectivity of **27** may be explained by a fast inactivation of JAK3 via covalent interaction before the highly reactive compound is decomposed in the DTT-containing kinase buffer. Based on these results the compounds with the most favorable isoform selectivities (compounds **11**, **23**, **27** and **28**) were selected for further evaluation in cellular assays and metabolic stability experiments.

Table 2. JAK isoform selectivity for chosen compounds.

	IC_{50} [nM][a]			
Compd.	**JAK1**	**JAK2**	**JAK3**	**TYK2**
1	0.50	2	0.29	9
2	344	578	1	2110[b]
8	19	113	22	78
11	12	53	0.21	44
17	45	183	48	139
20	16	48	10	25

23	52	346	0.13	459
	668[c]	3460[b,c]	2[c]	11800[b,c]
27[d]	4	188	0.39	14
28	117	765	0.74	791

[a]IC_{50} values were calculated from the results of a radiometric assay. Data were obtained as 5-dose singlicate IC_{50} with 10-fold serial dilution starting at 1 μM. [ATP] = 10 μM [b]starting concentration 50 μM [c][ATP] = 200 μM [d]arylidene dinitriles show unspecific reactivity with assay buffer components.

Cellular Activity and Target Engagement. We used different assay types to assess JAK3 inhibitory potency and selectivity of the selected compounds in a cellular setting. First we used a NanoBRET assay system to demonstrate target engagement and to confirm isoform selectivity on full length Janus kinases in cells.[33] This assay system utilizes ectopically expressed nano-luciferase-tagged full-length kinases, which interact with a fluorescent-labelled tracer-molecule binding to the ATP binding site. While the tracer is bound to the kinase, the spatial proximity of the luciferase and the fluorescence dye results in a measurable optical signal via bioluminescence resonance energy transfer (BRET) upon substrate addition. The luminescence signal is diminished when the tracer is replaced from the ATP binding site by increasing concentrations of the tested inhibitor, hence allowing the determination of EC_{50} values on full-length kinases in cellular environments. We perfomed these assays for JAK1, JAK2 and JAK3 to confirm isoform selectivity and additionally for Bruton's tyrosine kinase (BTK), which is a likely off target of covalent JAK3 inhibitors since it possesses a cysteine at an equivalent position to C909 in JAK3.[18-19] For compounds **23** and **28**, which showed the best selectivity profiles within the JAK family (Table 2), isoform selectivity was confirmed in the cellular environment. While JAK3 EC_{50} values of 237 nM and 257 nM, respectively, were observed, the activities of the other two JAK isoforms, JAK1 and JAK2, were not influenced up to inhibitor concentrations of 10 μM

(Figure 5 and Table 3). Inhibition of BTK was detected only at very high concentrations of **28** (above 50 μM) but not for compound **23**, which is in accordance with the kinome selectivity data reported previously. For compounds **11** and **27** the JAK3 EC_{50} values shifted to the higher nanomolar range in this cellular assay (745 nM and 670 nM, respectively, Figure 5 and Table 3), suggesting a lower permeability for **11** and **27** when comparing these data to the IC_{50} values on the isolated enzyme (Table 1). While **11** still shows no significant binding to JAK1, it only exhibits a less pronounced 10-fold selectivity over JAK2. On the other hand, the arylidene dinitrile **27** demonstrated an only 10-fold selectivity over JAK1, while it hits JAK2 with a similar potency than JAK3 (EC_{50} = 0,63 μM, Table 3). Compared to the cyanoacrylamides **23** and **28**, these compounds show a slightly higher affinity towards BTK with EC_{50} values of 13.3 μM and 5.8 μM for **11** and **27**, respectively. The observed BTK selectivity of the tested compounds may be achieved by the residue inducing the arginine pocket. As we reported earlier,[27] none of the ten other human kinases with a cysteine equivalent to C909 in JAK3 possesses an arginine at the position of R911, which may be a mandatory requirement for the induction of this cavity. The slightly less pronounced selectivity of acrylonitrile **11** compared to cyanoacrylamides **23** and **28** may be explained by the missing covalent interaction to C909 as shown by the X-ray experiments described above. In summary, these data clearly demonstrated cellular target engagement along with a high selectivity for JAK3 for the cyanoacrylamide based inhibitors.

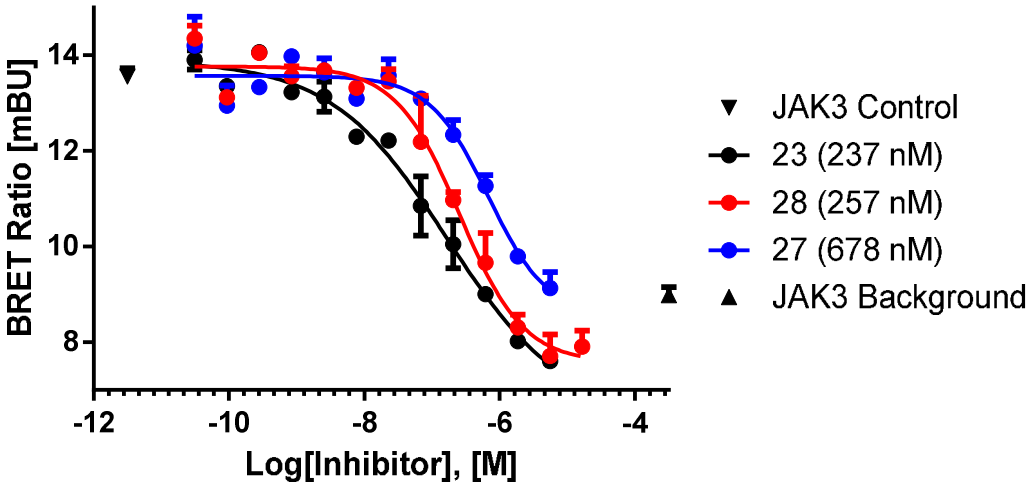

Figure 5. Representative BRET data measured on JAK3 kinase.

Table 3: Cellular EC_{50} values determined by nanoBRET.

	EC_{50} [nM][a]			
Compd.	**JAK1**	**JAK2**	**JAK3**	**BTK**
11	> 10 000	7710	740	13 300
23	> 10 000	> 10 000	237	> 10 000
27	7660	630	678	5790
28	> 10 000	> 10 000	257	> 10 000

[a]Values were calculated form a non-linear least square fit using BRET ratios measured at 11 different inhibitor concentrations.

To study the effect of our compounds on the JAK/STAT pathway in a physiologically more relevant model, we measured the dose dependent inhibition of STAT phosphorylation in primary human T-cells. Therefore, $CD4^+$ T-cells were incubated with increasing compound

concentrations and stimulated with different cytokines that associate with certain JAKs. The STAT phosphorylation levels were determined by immunoblotting after cell lysis (Figure 6).

We previously reported the results of **1** in this assay[27] and confirmed the panJAK inhibitory activity of this reference compound.[34] While **1** diminished the JAK1 and JAK3 dependent STAT phosphorylations after IL-2 or IL-4 stimulation in concentrations between 50 and 300 nM, it also decreased JAK1/JAK2/TYK2 dependent signaling at concentrations above 300 nM. Compound **2** only showed an effect on JAK mediated signaling after stimulation with IL-2 indicated by a weak inhibition of STAT5 phosphorylation at a concentration of 300 nM, while no effect was seen at concentrations up to 1 μM after stimulation with the three other cytokines. This rather low cellular activities are consistent with the previously described data for this reference compound, which initially seeded the controversial conclusion that JAK1 has a dominant role over JAK3.[9, 16]

The putative reversible acrylonitrile-derived inhibitor **11** showed a moderate JAK3 selectivity significantly inhibiting the JAK3-dependent phosphorylations of STAT5 and STAT6 with concentrations from 100 to 300 nM (Figure 6 A+B) while IFN-α induced STAT1 phosphorylation was only weakly inhibited at 1000 nM and IL-6 dependent pSTAT3 levels were not decreased at the same concentration (Figure 6 C+D).

The arylidene dinitrile **27** exhibited a somewhat weaker inhibition of the JAK1/3 dependent STAT phosphorylation with a significant inhibition of IL-2 signaling but no effect on the IL-4 triggered pathway at the highest tested concentration of 300 nM (Figure 6 A+B). Since **27** showed significant binding to JAK2 in the BRET assays (Table 3) it is not surprising that it also weakly inhibited JAK1/JAK2/TYK2-dependent STAT3 phosphorylation at the highest concentration of 1000 nM, while sparing JAK1/TYK2-dependent STAT1 phosphorylation

(Figure 6 C+D). It should be noted, that despite the aforementioned unselective thiol reactivity, compound **27** is still able to achieve a weak but evident selectivity for the inhibition of JAK3-dependent signaling pathways in this functional cell assay.

A more pronounced JAK3 selectivity was demonstrated for cyanoacrylamides **23**[27] and **28** showing significant inhibition of IL-2 induced STAT5 phosphorylation at concentrations around 50 to 100 nM (Figure 6 A) and blockade or reduction of IL-4 induced STAT6 phosphorylation at concentrations around 300 nM (Figure 6 B). At the same time, the JAK3-independent IL-6 and IFN-α pathways are not influenced by **23** and **28** even at concentrations up to 1000 nM (Figure 6 C+D). These results are in good agreement to the initially shown cellular selectivity from the BRET assays (Table 3) and the outcome from these stimulation experiments demonstrates in a semi-quantitative manner that highly selective JAK3 inhibition is sufficient to effectively abrogate the downstream signaling of γ_c cytokines.

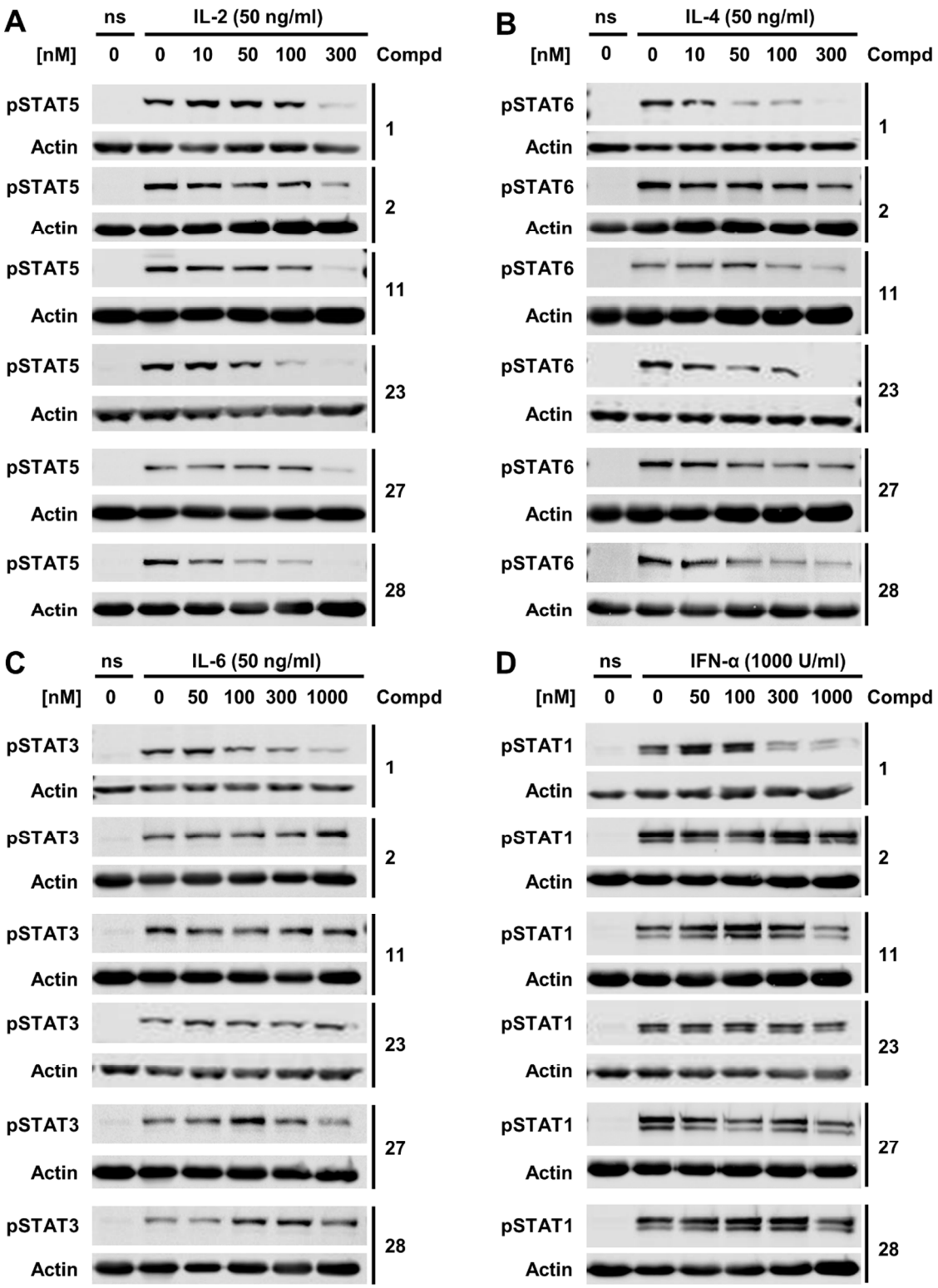

Figure 6. Inhibition of cytokine-induced STAT-phosphorylation of selected compounds. Human $CD4^+$ T-cells were incubated with the indicated concentrations of **1**, **2**, **11**, **23**, **27** or **28** for one

hour followed by 30 min stimulation with single cytokines. The cells were lysed and the pSTAT levels were determined via immunoblotting. Actin was co-blotted to ensure equal loadings IL-2 activates JAK1/3 dependent STAT5 phosphorylation (A), IL-4 activates JAK1/3 dependent STAT6 phosphorylation (B), IL-6 activates JAK1/JAK2/TYK2 dependent STAT3 phosphorylation (C) and IFN-α activates JAK1/TYK2 dependent STAT1 phosphorylation (D). The cellular assays/immunoblots for **1** and **23** were performed in a separate experiment as published previously[26] than the tests/blots for **2**, **11**, **27** and **28**.

Table 4. *in vitro* stability and solubility of selected compounds.

Compound	MLM stability[a] [%] ± SD	HWB stability[b] [%] ± SD	aqueous solubility[c] [mg/l] / [μM]
11	53.9 ± 2.1	98.8 ± 3.6	n.d.[d]
23	58.0 ± 0.9	49.4 ± 1.7	24 / 56
27	11.0 ± 0.7	1.5 ± 0.1	n.d.[d]
28	6.9 ± 3.9	47.0 ± 1.2	120 / 248

[a]percentage of residual compound after 180 min incubation with mouse liver microsomes. [b]percentage of residual compound after 180 min incubation with human whole blood. [c]aqueous solubility in PBS puffer pH 7.4 [d]n.d. = not determined.

Solubility and Metabolic Stability. Aiming for an *in vivo* use of our new JAK3 probes, we next focused on physicochemical and metabolic properties of selected compounds. During the work on this structure class, we recognized that the developed inhibitors showed limited solubility. Indeed, the aqueous solubility of key compound **23** determined in phosphate buffered saline (PBS) at a physiological pH of 7.4 proved to be fairly low (24 mg/l or 56 μM, respectively). An improved solubility was achieved by replacing the dimethyl amide residue by a more polar *N*-methylpiperazine amide (compound **28**), which would be protonated under physiological conditions. Since this residue is not responsible for critical interactions with the

kinase, this transformation maintained the good potency and selectivity as described before (Table 1 and 2) while resulting in a 5-fold increase in aqueous solubility to 120 mg/l or 248 µM, respectively (Table 4).

The *in vitro* stability of the compounds **11**, **23**, **27** and **28** was tested in mouse liver microsomes (MLM) as well as in human whole blood (HWB). While compounds **27** and **28** undergo fast degradation in the microsomal stability assay with only a small amount (ca. 10 %) remaining intact at the three-hour end point, compounds **11** and **23** showed a favorable microsomal stability with more than 50 % of the parent compound remaining after three hours of incubation (Table 3). Mass spectrometric analysis of the metabolites suggested the main metabolic transformations to be hydroxylation, hydrolysis of the nitrile to an amide and dealkylation of the cyclohexyl sidechain or the amide residues of **23** and **28**. The fast decomposition of **28** is probably due to the cleavage of the metabolically vulnerable *N*-methylpiperazine moiety, which most probably undergoes demethylation as well as ring opening. Since this moiety is not required for critical interactions to the kinase, the metabolites originating from transformation of the piperazine ring are likely to retain JAK3 inhibitory activity. However, this remains speculative since the identification of possible metabolites of **28** and the determination of their biological activity were not within the scope of this study.

To assess the general stability of the electrophilic inhibitors in a medium with a high content of endogenous nucleophiles, we incubated the compounds with human whole blood (HWB) and determined the residual amount of parent compound after three hours via mass spectrometry. As in the microsomal stability assay, the arylidendinitrile **27** demonstrated a very low stability under these conditions with only 1.5 % of the parent substance left after 3 h of incubation. This poor overall stability of **27** can be most probably attributed to the very high electrophilicity of the

dinitrile Michael system and the high intrinsic reactivity of this functional group. In contrast, the simple acrylonitrile **11** showed a good stability in the HWB assay and was only marginally degraded at the three-hour end-point of the stability assay (Table 4). Cyanoacrylamides **23** and **28** both demonstrated a lower but still favorable whole blood stability with a half-life of around three hours (Table 4).

Since key compound **23** exhibited favorable stability in both assays combined with an excellent JAK3 potency and selectivity, we consider it the most promising candidate for *in vivo* studies within this inhibitor class.

Scheme 1. Synthesis of JAK inhibitors 3-28[a]

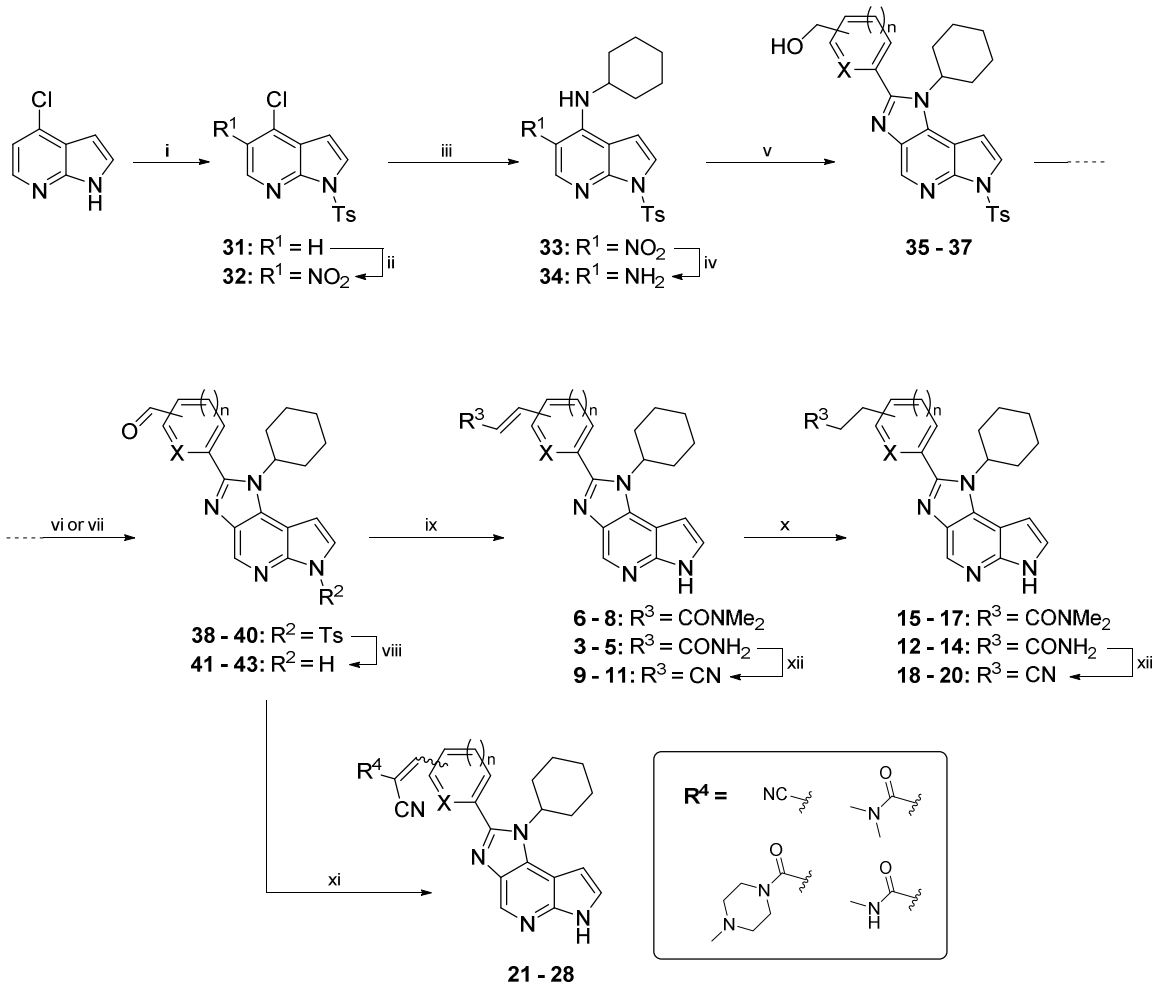

[a](i) NaH, TsCl, THF, 0 °C to rt, 93%; (ii) $Me_4N{\cdot}NO_3$, TFAA, DCM, 0-5 °C, 67%; (iii) cyclohexylamine, Et_3N, *i*PrOH, reflux, 94%; (iv) Pd/C, H_2, MeOH / EtOAc, 50 °C, quant; (v) corresponding aldehyde, $KHSO_5$, DMF / H_2O, rt, 68-72%; (vi) DMP, DCM, rt, 80-92%; (vii) $Cu(MeCN)_4{\cdot}OTf$, TEMPO, bpy, NMI, O_2, MeCN, 50 °C, 87%; (viii) KOH, MeOH, rt, 54-75% (ix) corresponding HWE-reagent, LiCl, DBU, MeCN / $CHCl_3$, 54-88%; (x) Pd/C, H_2, MeOH / EtOAc, rt, 60-95%; (xi) corresponding cyanoacetamide or malononitrile, piperidine, MeOH, 60 °C, 20-93% (xii) cyanuric chloride, DMF, rt, 50-81%

CHEMISTRY. We previously reported a synthesis of **23**[27] which was slightly modified to allow a more convenient access to gram quantities of key intermediates and final compounds. The synthetic route to compounds **3-28** is shown in Scheme 1 and starts from commercially available 4-chloro-1*H*-pyrrolo[2,3-*b*]pyridine. After tosyl protection and nitration in position 5 under mild anhydrous conditions, the cyclohexyl sidechain was introduced via a nucleophilic aromatic substitution. Catalytic hydrogenation afforded key intermediate **34**, which is unsuitable for long term storage under ambient conditions and should be used in the next step immediately. Closure of the imidazole ring was achieved by condensation with the corresponding aldehydes under oxidative conditions in wet DMF.[35] Benzylic alcohols **35** and **36** were initially transformed to the corresponding aryl carbaldehydes **38** and **39** via Dess-Martin-Oxidation.[36] However, since this reaction can be problematic on a multigram scale it was replaced by a catalytic Stahl-Oxidation[37] for the conversion of furan derivative **37** to aldehyde **40**. Intermediates **41-43** were obtained by tosyl cleavage with methanolic KOH at ambient temperature. Acrylamides **3-8** were accessible via a LiCl-promoted Horner-Wadsworth-Emmons (HWE) reaction according to a protocol modified from Blanchette *et al*.[38] The saturated analogues were prepared from the corresponding acrylamides by catalytic hydrogenation on Pd/C. Nitriles **9-11** and **18-20** were synthesized from the corresponding primary amides by dehydration with cyanuric chloride in DMF.[39] Cyanoacrylamide- and malononitrile-derived inhibitors **21-28** were obtained from aldehydes **41-43** under Knoevenagel conditions with the corresponding cyanoacetamides or

malononitrile. The cyanoacetamides for the synthesis of **24** and **28** were obtained via aminolysis of ethyl cyanoacetate (see Supporting Information). Compound **29** was synthesized following the same procedures described in Scheme 1, but using aqueous methylamine solution instead of cyclohexylamine for S_NAr (see Supporting Information for detailed procedures). Methylated compound **30** was prepared by reacting **23** with methyl iodide after deprotonation with NaH in DMF (see Supporting Information).

CONCLUSION:

Herein we report our efforts to elucidate the role of a ligand-induced binding pocket in JAK3 formed by interactions of arginine residues with a nitrile substituent, which was initially observed for cyanoacrylamide-based inhibitors. Our recently described covalent-reversible inhibitor **23**[27] was iteratively modified to establish detailed SARs regarding this previously unknown "arginine pocket" and we were able to show a correlation between inhibitor selectivity and the formation of this cavity. With compound **11** we demonstrated via X-ray crystallography and *in vitro* profiling that a significant JAK3 selectivity can be achieved by induction of the arginine pocket even without covalent bond formation to the JAK3-specific C909. The application of nitrile-bearing covalent-reversible warheads resulted in a positive synergism of both selectivity vectors and yielded a set of JAK3 inhibitors with an extraordinarily high potency and isoform selectivity. The favorable selectivity profile of the compounds **11**, **23**, **27** and **28** was further validated in several cellular assays demonstrating target engagement in engineered cells as well as selective inhibition of JAK3 dependent downstream signaling in functional human T-cells. Our data also indicate that a highly selective inhibition of JAK3 is sufficient to abrogate JAK1/3 dependent STAT-phosphorylation without the need of a simultaneous JAK1 inhibition. This is in good agreement with recent data from other groups, who investigated this issue and

even provided some *in vivo* data.[20, 26, 40] Compound **23** exhibited an acceptable stability profile in two *in vitro* metabolism assays, while bioavailability remains to be shown. These studies are ongoing and will be published in due course. In summary, our SAR study revealed that the well characterized cyanoacrylamide **23** is currently the most optimized candidate from this series. This compound is a promising tool, complementing the existing irreversible acrylamide-based inhibitors by a covalent-reversible mode of action and may be suitable to investigate the effects of highly selective JAK3 inhibition in *in vivo*.

EXPERIMENTAL SECTION:

Protein expression and structure determination: Recombinant JAK3 was purified as previously described.[27] The protein was mixed with 1 mM inhibitors and 0.26% N-phenylurea. Crystallization was performed using sitting-drop vapor diffusion method at 4 °C and the reservoir solution containing 24-30% PEG 3350, 0.1 M MES, pH 5.5-6.0 and 0.1-0.2 M $MgCl_2$. Diffraction data were collected at Diamond Light Source, beamline i03 using X-ray at wavelength of 0.97623 Å, and were processed and scaled with XDS and Scala, respectively.[41-42] Structure solutions were obtained by molecular replacement method using Phaser[43] and the published JAK3 coordinates.[27] Manual Model rebuilding alternated with refinement were performed in COOT and REFMAC.[44-45] Geometric correctness was verified using MOLPROBITY.[46] The data collection and refinement statistics are summarized in Supplemental Table S1. Visualization of X-ray crystallographic data and preparation of images was performed with PyMol.[47]

JAK1/2/3 and BTK NanoBRET Assays: Assays were performed essentially as described previously.[27] In brief: Full-length JAK1, JAK2, JAK3 and BTK ORF (Promega) cloned in frame with a C-terminal NanoLuc-fusion were transfected into HEK cells and proteins were allowed to

express for 20h. Serially diluted inhibitor and NanoBRET Kinase Tracer-04 (Promega) at 1 μM for JAK1, Tracer-05 (Promega) at 2 μM for JAK2/JAK3 and at 1 μM for BTK, respectively, were pipetted into white 384-well plates (Greiner 781 207). The corresponding JAK1/JAK2/JAK3 or BTK-transfected cells were added and reseeded at a density of 2 x 105 cells per well after trypsinization and resuspending in Opti-MEM without phenol red (Life Technologies). The system was allowed to equilibrate for 2 hours at 37°C/5% CO2 prior to BRET measurements. To measure BRET, NanoBRET NanoGlo Substrate + Extracellular NanoLuc Inhibitor (Promega) was added as per the manufacturer's protocol, and filtered luminescence was measured on a CLARIOstar plate reader (BMG Labtech) equipped with 450 nm BP filter (donor) and 610 nm LP filter (acceptor). Competitive displacement data were then graphed using GraphPad Prism software using a 4-parameter curve fit with the following equation:

Y=Bottom + (Top-Bottom) / (1+10^((LogIC50-X)*HillSlope))

$CD4^+$ T-cell stimulations: The stimulation experiments were carried out following the same procedure reported previously.[27] $CD4^+$ T cells were purified from human PBMCs using magnetic cell separation technology (Miltenyi Biotec) followed by activation with plate-bound anti-CD3 (clone UCHT1) and anti-CD28 (clone CD28.2) antibodies (each 5 μg/ml, Biolegend) in XVIVO 15 medium (Lonza) for 3 days and expanded with rhIL-2 for another 6 days. After expansion T cells were washed and rested in fresh medium overnight. Equal numbers of T cells were incubated with the indicated concentrations of compounds **1**, **2**, **11**, **23**, **27** and **28** in DMSO or DMSO alone (control) for 1 hour and then stimulated with either rhIL-2 (50 ng/ml; Proleukin, Novartis), rhIL-6 (50 ng/ml; Peprotech), rhIL-4 (50 ng/ml, Peprotech) or IFN-α (1000 U/ml, Roche) for 30 min. After stimulation, cells were lysed in Triton X-100 lysis buffer containing

protease and phosphatase inhibitors. Equal amounts of total protein were separated by PAGE, transferred to PVDF membrane, and blotted with Abs recognizing actin (Merck Millipore), specific phospho-STAT antibodies (anti-phospho-Stat5 Tyr694, antiphospho-Stat3 Tyr705, both Cell Signaling) and IRDye-labelled secondary antibodies (680RD, 800CW, both LI-COR Biosciences) for detection. Specific bands were visualized using an Odyssey infrared imaging system (LI-COR Biosciences).

MLM Stability: Murine liver microsomes (1 mg/ml), a NADPH-regenerating system (5 mM glucose-6-phosphate, 5 U/ml glucose-6-phosphate-dehydrogenase and 1 mM $NADP^+$) and 4 mM $MgCl_2$ in 0,1 M Tris-buffer (pH = 7.4) were preincubated for 5 min at 37 °C. The reaction was started by addition of the analyte (100 µM) and incubation was continued at 37 °C. At defined time points 50 µL aliquots were quenched by addition of a precooled solution of 100 µl internal standard (100 µM) in MeCN. The samples were vortexed, sonicated for 30 min and centrifugated. The supernatant was directly used for quantitative determination via LC-MS.

HWB stability: Determination of human whole blood stability was carried out following a similar procedure described previously by Thorarensen *et al.*[26] Fresh human whole blood (EDTA) from two healthy male subjects were incubated at 37 °C followed by addition of the analytes to a final concentration of 1 µM. Incubation was continued at 37 °C and 100 µl aliquots were quenched at defined time points by addition to a precooled solution of internal standard (100 µM) in MeCN. The samples were vortexed, sonicated for 30 min and centrifugated. The supernatant was directly used for quantitative determination via LC-MS.

Solubility determination: The solubility of compounds **23** and **28** were determined via standard HPLC techniques. A linear calibration curve was determined in MeOH from seven different concentrations starting from 1,0 mg/ml with two-fold serial dilution steps. AUCs from

HPLC runs using the same method as described below were plotted against the concentration and the calibration curve was set up via linear regression. Samples of **23** and **28** were prepared by stirring excess of solid material in 0.05 M PBS buffer pH 7,4 overnight at ambient temperature. The samples were centrifuged and the supernatant analyzed by HPLC. With the obtained AUC, the aqueous solubility was calculated using the compound specific calibration curve.

General: Reagents, starting materials and solvents were of commercial quality and were used without further purification unless otherwise stated. HWE reagents and hydroxybenzaldehydes were synthesized as reported earlier.[27] For the preparation of cyanoacetamides and compounds **29** and **30**, see Supplementary Information. TLC analysis was carried out on Merck 60 F254 silica gel plates and visualized under UV light at 254 nm and 365 nm. Preparative column chromatography was carried out on Grace Davison Davisil LC60A 20-45 micron or Merck Geduran Si60 63-200 micron silica using a Interchim PuriFlash 430 automated flash chromatography system. The purity of final compounds was determined via RP-HPLC on a Hewlett Packard 1090 Series II LC or an Agilent 1100 Series LC with Phenomenex Luna C8 columns (150 x 4.6 mm, 5 µm) and detection was performed with a UV DAD at 254 nm and 230 nm wavelength. Elution was carried out with the following gradient: 0.01 M KH2PO4, pH 2.30 (solvent A), MeOH (solvent B), 40 % B to 85 % B in 8 min, 85 % B for 5 min, 85 % to 40 % B in 1 min, 40 % B for 2 min, stop time 16 min, flow 1.5 ml/min. NMR spectra were recorded on a Bruker Avance 200 or Bruker Avance 400 NMR spectrometer. Chemical shifts are reported in ppm relative to TMS and the spectra were calibrated against the residual proton peak of the used deuterated solvent. Standard mass spectra were obtained either as ESI-MS (pos. and/or neg. mode) from a Advion DCMS interface, (settings as follows: ESI voltage 3,50 kV, capillary voltage 187 V, source voltage 44 V, capillary temperature 250 °C, desolvation gas

temperature 250 °C, gas flow 5 l/min) or as FAB-MS (pos. and/or neg. mode) measured by the mass spectrometry department, Institute of Organic Chemistry, Eberhard-Karls-University Tuebingen. HRMS for final compounds were measured by the mass spectrometry department, Institute of Organic Chemistry, Eberhard-Karls-University Tuebingen on a Bruker maXis 4G ESI-TOF from Daltonik/Bremen. The instrument was run in ESI+ Mode, settings were as follows: nebulizer gas 1.2 bar, gas flow, 6.0 l/min, source temperature 200 °C, capillary voltage +4500 V, end plate offset -500 V. m/z range from 80 to 1000 m/z. All final compounds show ≥ 95 % purity according to analytical HPLC. The biologically active compounds were screened for known patterns of assay interference compounds using the ZINC15 database.[48] This analysis revealed potential interference potential for the structural element of the arylidene dinitriles (compounds **25-27**). The issue of the high intrinsic electrophilicity of these compounds was already discussed above and the evident JAK3 selectivity of the representative compound **27** in different biochemical and cellular assays demonstrates that the biological activity of these compound class is not only an artifact.

General Procedure A for HWE-Reaction to Acrylamides 3-8. To a suspension of LiCl (1.5 eq) in dry MeCN (0.2 M) was added appropriate HWE-reagent (1.5 eq) and DBU (1.5 eq). The mixture was stirred for 10 min at ambient temperature before **41**, **42** or **43** was added as suspension in dry chloroform (ca. 0.8 M). The reaction was monitored via TLC and quenched with sat. NH_4Cl after complete conversion. After extractive workup with DCM (5x) the combined organics were dried over Na_2SO_4 and evaporated. The crude product was purified via flash chromatography unless otherwise stated.

(E)-3-(4-(1-Cyclohexyl-1,6-dihydroimidazo[4,5-d]pyrrolo[2,3-b]pyridin-2-yl)phenyl)acrylamide (3) was obtained from 200 mg **41** and 170 mg diethyl (2-amino-2-

oxoethyl)phosphonate following general procedure D but with alternative workup procedure. The product precipitated out of solution and showed bad solubility in common organic solvents like DCM and EtOAc. The crude product was isolated by filtration and was subjected to column chromatography with DCM / MeOH (8 - 20%), which resulted in a bad elution. The combined product fractions still contained considerable amounts of HWE-reagent, which were removed by washing with water. Yield: 120 mg (54 %) of **3** as yellowish solid. ^{1}H NMR (400 MHz, DMSO) δ 11.98 (br s, 1H), 8.64 (s, 1H), 7.75 (dd, *J* = 19.6, 8.3 Hz, 4H), 7.63 (br s, 1H), 7.57 – 7.48 (m, 2H), 7.21 (br s, 1H), 6.82 – 6.78 (m, 1H), 6.75 (d, *J* = 15.9 Hz, 1H), 4.47 – 4.35 (m, 1H), 2.45 – 2.30 (m, 2H), 1.98 – 1.86 (m, 4H), 1.77 – 1.68 (m, 1H), 1.50 – 1.29 (m, 3H); ^{13}C NMR (100 MHz, DMSO) δ 166.4, 151.0, 144.4, 138.2, 136.0, 135.8, 134.8, 132.5, 131.6, 130.0, 127.7, 123.9, 123.7, 104.2, 100.0, 56.0, 30.3, 25.1, 24.3. ESI-HRMS $[M+H]^+$ calculated for $C_{23}H_{23}N_5O$: 386.19754, found: 386.19758 HPLC t_{ret} = 6.730 min

(E)-3-(3-(1-Cyclohexyl-1,6-dihydroimidazo[4,5-d]pyrrolo[2,3-b]pyridin-2-yl)phenyl)acrylamide (4) was obtained from 55 mg **42** and 22 mg diethyl (2-amino-2-oxoethyl)phosphonate following general procedure D with a reaction time of two hours at ambient temperature. Flash purification with DCM / MeOH (8 – 16%). Yield: 22 mg (78 %) of **4** as off-white solid. ^{1}H NMR (200 MHz, DMSO) δ 11.97 (br s, 1H), 8.65 (s, 1H), 7.87 (s, 1H), 7.82 – 7.45 (m, 6H), 7.18 (s, 1H), 6.86 – 6.68 (m, 2H), 4.52 – 4.26 (m, 1H), 2.44 – 2.22 (m, 2H), 2.07 – 1.64 (m, 5H), 1.53 – 1.25 (m, 3H). ^{13}C NMR (50 MHz, DMSO) δ 166.5, 151.1, 144.5, 138.4, 135.8, 135.4, 134.8, 132.4, 131.6, 130.2, 129.4, 128.7, 128.5, 124.0, 123.5, 104.3, 100.0, 56.1, 30.3, 25.2, 24.3. ESI-HRMS $[M+H]^+$ calculated for $C_{23}H_{23}N_5O$: 386.19754, found: 386.19788 HPLC t_{ret} = 6.341 min

(E)-3-(5-(1-Cyclohexyl-1,6-dihydroimidazo[4,5-d]pyrrolo[2,3-b]pyridin-2-yl)furan-2-yl)acrylamide (5) was obtained from 120 mg **43** and 105 mg diethyl (2-amino-2-oxoethyl)phosphonate following general procedure A with a reaction time of two hours at ambient temperature. Extraction was performed with EtOAc instead of DCM. Flash purification with DCM / MeOH (4 – 18%). Yield: 105 mg (78 %) of **5** as yellowish solid. ^{1}H NMR (200 MHz, DMSO) δ 12.04 (br s, 1H), 8.66 (s, 1H), 7.73 (br s, 1H), 7.59 – 7.50 (m, 1H), 7.36 (d, *J* = 15.7 Hz, 1H), 7.25 – 7.13 (m, *J* = 3.6 Hz, 2H), 7.04 (d, *J* = 3.7 Hz, 1H), 6.85 – 6.76 (m, 1H), 6.56 (d, *J* = 15.7 Hz, 1H), 4.97 – 4.71 (m, 1H), 2.47 – 2.19 (m, 2H), 2.06 – 1.84 (m, 4H), 1.83 – 1.68 (m, 1H), 1.63 – 1.37 (m, 3H); ^{13}C NMR (50 MHz, DMSO) δ 166.2, 152.1, 145.3, 144.6, 141.4, 136.1, 134.8, 132.7, 126.1, 124.1, 121.1, 115.4, 115.0, 104.2, 99.9, 56.4, 30.3, 25.3, 24.4. ESI-HRMS $[M+H]^+$ calculated for $C_{21}H_{21}N_5O_2$: 376.17680, found: 376.17721 HPLC t_{ret} = 6.741 min

(E)-3-(4-(1-Cyclohexyl-1,6-dihydroimidazo[4,5-d]pyrrolo[2,3-b]pyridin-2-yl)phenyl)-N,N-dimethylacrylamide (6) was obtained from 50 mg **41** and 49 mg diethyl (2-(dimethylamino)-2-oxoethyl)phosphonate following general procedure A with a reaction time of four hours at ambient temperature. Flash purification with DCM / MeOH (4 – 10%). Yield: 42 mg (70 %) of **6** as white solid. ^{1}H NMR (200 MHz, $CDCl_3$ + MeOD) δ 8.77 (s, 1H), 7.80 – 7.59 (m, 5H), 7.41 (d, *J* = 3.6 Hz, 1H), 6.99 (d, *J* = 15.5 Hz, 1H), 6.84 (d, *J* = 3.6 Hz, 1H), 4.47 (tt, *J* = 12.3, 4.3 Hz, 1H), 3.13 (d, *J* = 24.8 Hz, 6H), 2.63 – 2.40 (m, 2H), 2.06 – 1.74 (m, 5H), 1.55 – 1.30 (m, 3H). indole NH was exchanged by MeOD but residual peak was visible with 0.2 protons. ^{13}C NMR (50 MHz, $CDCl_3$ + MeOD) δ 167.2, 152.7, 144.9, 141.9, 137.2, 136.6, 135.7, 134.1, 132.3, 130.4, 128.5, 123.6, 119.2, 105.5, 101.2, 56.7, 37.4, 35.9, 30.7, 25.4, 24.5 ESI-HRMS $[M+H]^+$ calculated for $C_{25}H_{27}N_5O$: 414.22884, found: 414.22919 HPLC t_{ret} = 6.938 min

(E)-3-(3-(1-Cyclohexyl-1,6-dihydroimidazo[4,5-d]pyrrolo[2,3-b]pyridin-2-yl)phenyl)-N,N-dimethylacrylamide (7) was obtained from 26 mg **42** and 25 mg (2-(dimethylamino)-2-oxoethyl)phosphonate following general procedure A with a reaction time of two hours at ambient temperature. Flash purification with DCM / MeOH (3 – 10%). Yield: 23 mg (74 %) of **7** as off-white solid. ^{1}H NMR (200 MHz, $CDCl_3$) δ 11.70 (br s, 1H), 8.89 (s, 1H), 7.89 (s, 1H), 7.81 – 7.43 (m, 5H), 7.00 (d, *J* = 15.5 Hz, 1H), 6.88 (d, *J* = 3.3 Hz, 1H), 4.61 – 4.36 (m, 1H), 3.12 (d, *J* = 19.3 Hz, 6H), 2.62 – 2.35 (m, 2H), 2.08 – 1.71 (m, 5H), 1.62 – 1.32 (m, 3H). ^{13}C NMR (50 MHz, $CDCl_3$) δ 166.5, 152.4, 144.5, 141.4, 136.3, 136.0, 135.4, 133.9, 131.8, 130.3, 129.6, 129.3, 128.6, 123.4, 119.0, 105.5, 101.1, 56.9, 37.6, 36.1, 31.1, 25.8, 24.9 ESI-HRMS $[M+H]^+$ calculated for $C_{25}H_{27}N_5O$: 414.22884, found: 414.22874 HPLC t_{ret} = 6.636 min

(E)-3-(5-(1-Cyclohexyl-1,6-dihydroimidazo[4,5-d]pyrrolo[2,3-b]pyridin-2-yl)furan-2-yl)-N,N-dimethylacrylamide (8) was obtained from 40 mg **43** and 41 mg (2-(dimethylamino)-2-oxoethyl)phosphonate following general procedure A with a reaction time of two hours at ambient temperature. Flash purification with DCM / MeOH (4-10%). Yield: 42 mg (88 %) of **8** as slightly yellowish solid. ^{1}H NMR (200 MHz, $CDCl_3$) δ 11.92 (br s, 1H), 8.88 (s, 1H), 7.55 (d, *J* = 15.2 Hz, 1H), 7.49 (d, *J* = 3.5 Hz, 1H), 7.10 (d, *J* = 3.6 Hz, 1H), 6.94 (d, *J* = 15.2 Hz, 1H), 6.86 (d, *J* = 3.5 Hz, 1H), 6.75 (d, *J* = 3.6 Hz, 1H), 5.09 – 4.84 (m, 1H), 3.12 (d, *J* = 17.1 Hz, 6H), 2.67 – 2.35 (m, 2H), 2.18 – 1.78 (m, 5H), 1.64 – 1.37 (m, 3H). ^{13}C NMR (50 MHz, $CDCl_3$) δ 166.8, 153.5, 146.6, 145.4, 143.1, 136.9, 136.0, 134.4, 129.1, 123.7, 116.7, 115.7, 115.4, 105.4, 101.0, 57.2, 37.2, 35.9, 30.6, 25.7, 24.7 ESI-HRMS $[M+H]^+$ calculated for $C_{23}H_{25}N_5O_2$: 404.20810, found: 404.20835 HPLC t_{ret} = 7.148 min

General Procedure B for Dehydration to Nitriles 9-11 and 18-20. Cyanuric chloride (1 eq) was dissolved in ice-cooled dry DMF and stirred for 10 min before primary amide (**3**, **4**, **5**, **12**, **13**

or **14**) was added dropwise as solution or suspension in dry DMF. After complete addition the mixture was stirred at the stated temperature until TLC indicated full consumption of starting material. Then the reaction was quenched with sat. $NaHCO_3$ and extracted with EtOAc (4x). The combined organic layers were washed with brine, dried over Na_2SO_4 and evaporated. The residue was purified via flash chromatography.

(E)-3-(4-(1-Cyclohexyl-1,6-dihydroimidazo[4,5-d]pyrrolo[2,3-b]pyridin-2-yl)phenyl)acrylonitrile (9) was prepared from 45 mg **3** as suspension in 3 ml DMF and 22 mg cyanuric chloride in 1 ml DMF following general procedure B with a reaction time of 30 min under ice-cooling. Flash purification with DCM / MeOH (4 - 10%). Yield: 34 mg (81 %) of **9** as white solid. ^{1}H NMR (400 MHz, DMSO) δ 12.02 (br s, 1H), 8.66 (s, 1H), 7.87 (d, *J* = 8.2 Hz, 2H), 7.83 – 7.72 (m, 3H), 7.55 (t, *J* = 2.9 Hz, 1H), 6.83 – 6.77 (m, 1H), 6.62 (d, *J* = 16.7 Hz, 1H), 4.45 – 4.32 (m, 1H), 2.43 – 2.29 (m, 2H), 2.00 – 1.85 (m, 4H), 1.76 – 1.67 (m, 1H), 1.51 – 1.28 (m, 3H); ^{13}C NMR (100 MHz, DMSO) δ 150.7, 149.7, 144.3, 135.7, 134.7, 134.7, 133.0, 132.5, 130.0, 127.9, 124.0, 118.6, 104.2, 100.0, 98.1, 56.1, 30.2, 25.0, 24.2. ESI-HRMS $[M+H]^+$ calculated for $C_{23}H_{21}N_5$: 368.18697, found: 368.18720 HPLC t_{ret} = 7.888 min

(E)-3-(3-(1-Cyclohexyl-1,6-dihydroimidazo[4,5-d]pyrrolo[2,3-b]pyridin-2-yl)phenyl)acrylonitrile (10) was prepared from 40 mg **4** as suspension in 1 ml DMF and 22 mg cyanuric chloride in 1 ml DMF following general procedure B with a reaction time of 40 min under ice-cooling. Flash purification with DCM / MeOH (4 - 10%). Yield: 30 mg (79 %) of **10** as yellow solid. ^{1}H NMR (400 MHz, $CDCl_3$) δ 11.84 (br s, 1H), 8.88 (s, 1H), 7.84 (s, 1H), 7.71 – 7.58 (m, 3H), 7.53 (d, *J* = 3.1 Hz, 1H), 7.47 (d, *J* = 16.7 Hz, 1H), 6.90 (d, *J* = 3.1 Hz, 1H), 6.00 (d, *J* = 16.7 Hz, 1H), 4.52 – 4.39 (m, 1H), 2.60 – 2.43 (m, 2H), 2.08 – 1.93 (m, 4H), 1.89 – 1.78 (m, 1H), 1.56 – 1.35 (m, 3H); ^{13}C NMR (100 MHz, $CDCl_3$) δ 152.1, 149.6, 143.8, 135.4, 135.3,

134.5, 134.4, 132.3, 131.8, 129.6, 128.8, 128.7, 123.8, 117.8, 105.7, 101.2, 98.2, 57.2, 31.1, 25.8, 24.9. ESI-HRMS $[M+H]^+$ calculated for $C_{23}H_{21}N_5$: 368.18697, found: 368.18717 HPLC t_{ret} = 7.879 min

(E)-3-(5-(1-Cyclohexyl-1,6-dihydroimidazo[4,5-d]pyrrolo[2,3-b]pyridin-2-yl)furan-2-yl)acrylonitrile (11) was prepared from 38 mg **5** as suspension in 2 ml DMF and 19 mg cyanuric chloride in 1 ml DMF following general procedure B with a reaction time of 30 min under ice-cooling. Flash purification with EtOAc / MeOH (0 - 15%). Yield: 24 mg (66 %) of **11** as yellow solid. ^{1}H NMR (400 MHz, DMSO) δ 12.06 (br s, 1H), 8.66 (s, 1H), 7.65 (d, *J* = 16.4 Hz, 1H), 7.58 – 7.52 (m, 1H), 7.26 (d, *J* = 3.6 Hz, 1H), 7.18 (d, *J* = 3.6 Hz, 1H), 6.84 – 6.78 (m, 1H), 6.09 (d, *J* = 16.4 Hz, 1H), 4.90 – 4.78 (m, 1H), 2.41 – 2.25 (m, 2H), 2.04 – 1.90 (m, 4H), 1.81 – 1.73 (m, 1H), 1.60 – 1.38 (m, 3H); ^{13}C NMR (100 MHz, DMSO) δ 150.7, 146.9, 144.6, 140.9, 136.3, 136.2, 134.9, 132.8, 124.1, 118.6, 117.7, 115.4, 104.1, 100.0, 94.3, 56.4, 30.3, 25.2, 24.4. ESI-HRMS $[M+H]^+$ calculated for $C_{21}H_{19}N_5O$: 358.16624, found: 358.16650 HPLC t_{ret} = 7.960 min

General Procedure C for Hydrogenation to Saturated Amides 12-17. To a solution of acrylamide (**3-8**) in the stated solvent mixture was added Pd/C (10 %wt Pd) and hydrogen was bubbled through the stirred solution for 5-10 min. Then the reaction was stirred under an atmosphere of hydrogen until reaction control indicated full conversion. The catalyst was filtered off, the filtrate evaporated and the residue purified via flash chromatography.

3-(4-(1-Cyclohexyl-1,6-dihydroimidazo[4,5-d]pyrrolo[2,3-b]pyridin-2-yl)phenyl)propanamide (12) was obtained from 58 mg **3** and 10 mg Pd/C in 20 ml DCM / MeOH (1:1) following general procedure C with stirring overnight at 40 °C oil-bath temperature. Product was sufficiently pure after filtering off the catalyst. Yield: 55 mg (95 %) of **12** as greyish solid. ^{1}H NMR (200 MHz, DMSO) δ 12.28 (br s, 1H), 8.75 (s, 1H), 7.73 – 7.56 (m, 3H), 7.53 –

7.31 (m, 3H), 6.99 – 6.67 (m, 2H), 4.56 – 4.30 (m, 1H), 2.95 (t, *J* = 7.3 Hz, 2H), 2.56 – 2.18 (m, 4H), 2.06 – 1.62 (m, 5H), 1.53 – 1.24 (m, 3H); ^{13}C NMR (50 MHz, DMSO) δ 173.7, 152.1, 144.5, 143.7, 133.6, 132.9, 132.4, 130.0, 129.1, 127.0, 125.4, 105.1, 100.7, 56.9, 36.5, 31.03, 30.4, 25.4, 24.6. ESI-HRMS $[M+H]^+$ calculated for $C_{23}H_{25}N_5O$: 388.21319, found: 388.21341 HPLC t_{ret} = 6.661 min

3-(3-(1-Cyclohexyl-1,6-dihydroimidazo[4,5-d]pyrrolo[2,3-b]pyridin-2-yl)phenyl)propanamide (13) was obtained from 14 mg **4** and 4 mg Pd/C in 2.5 ml THF / MeOH (4:1) following general procedure C with a reaction time of 90 min at ambient temperature. Flash chromatography with DCM / MeOH (8 – 16 %). Yield: 10 mg (71 %) of **13** as white solid. ^{1}H NMR (400 MHz, DMSO) δ 11.94 (s, 1H), 8.63 (s, 1H), 7.58 – 7.28 (m, 6H), 6.78 (s, 2H), 4.48 – 4.32 (m, 1H), 2.93 (t, *J* = 7.3 Hz, 2H), 2.45 (t, *J* = 7.3 Hz, 2H), 2.41 – 2.29 (m, 2H), 1.99 – 1.86 (m, 4H), 1.79 – 1.67 (m, 1H), 1.54 – 1.28 (m, 3H); ^{13}C NMR (100 MHz, DMSO) δ 173.2, 151.6, 144.4, 142.0, 135.7, 134.7, 132.3, 130.9, 129.6, 129.3, 128.6, 127.0, 123.8, 104.3, 99.9, 55.9, 36.4, 30.6, 30.3, 25.1, 24.3. ESI-HRMS $[M+H]^+$ calculated for $C_{23}H_{25}N_5O$: 388.21319, found: 388.21372 HPLC t_{ret} = 6.300 min

3-(5-(1-Cyclohexyl-1,6-dihydroimidazo[4,5-d]pyrrolo[2,3-b]pyridin-2-yl)furan-2-yl)propanamide (14) was obtained from 50 mg **5** and 10 mg Pd/C in 8 ml EtOAc / MeOH (1:1) following general procedure C with stirring overnight at 40 °C oil-bath temperature. Product was sufficiently pure after filtering off the catalyst. Yield: 45 mg (90 %) of **14** as yellowish solid. ^{1}H NMR (200 MHz, $CDCl_3$ + MeOD) δ 8.63 (s, 1H), 7.35 (d, *J* = 3.4 Hz, 1H), 6.84 – 6.67 (m, 2H), 6.24 (d, *J* = 3.4 Hz, 1H), 4.88 – 4.64 (m, 1H), 3.05 (t, *J* = 7.4 Hz, 2H), 2.62 (t, *J* = 7.4 Hz, 2H), 2.52 – 2.26 (m, 2H), 2.09 – 1.71 (m, 5H), 1.56 – 1.34 (m, 3H); ^{13}C NMR (50 MHz, $CDCl_3$ + MeOD) δ 174.9, 156.6, 143.9, 143.5, 142.4, 135.3, 134.5, 133.4, 123.3, 113.8, 108.0, 105.1,

100.6, 56.9, 33.3, 30.4, 25.6, 24.7, 24.0. ESI-HRMS $[M+H]^+$ calculated for $C_{21}H_{23}N_5O_2$: 378.19245, found: 378.19239 HPLC t_{ret} = 6.572 min

3-(4-(1-Cyclohexyl-1,6-dihydroimidazo[4,5-d]pyrrolo[2,3-b]pyridin-2-yl)phenyl)-N,N-dimethylpropanamide (15) was obtained from 16 mg **6** and 4 mg Pd/C in 5 ml EtOAc / MeOH (1:1) following general procedure C with a reaction time of one hour at ambient temperature. Flash chromatography with DCM / MeOH (4 – 10 %). Yield: 15 mg (93 %) of **15** as off-white solid. ^{1}H NMR (200 MHz, DMSO) δ 11.93 (bs, 1H), 8.62 (s, 1H), 7.63 – 7.39 (m, 5H), 6.78 (s, 1H), 4.51 – 4.28 (m, 1H), 2.99 – 2.80 (m, 8H), 2.69 (t, *J* = 7.2 Hz, 2H), 2.35 (m, 2H), 2.00 – 1.65 (m, 5H), 1.52 – 1.26 (m, 3H); ^{13}C NMR (50 MHz, DMSO) δ 171.2, 151.6, 144.4, 143.3, 135.7, 134.8, 132.4, 129.4, 128.8, 128.5, 123.9, 104.3, 100.1, 55.9, 36.7, 34.9, 33.7, 30.5, 30.3, 25.2, 24.3. ESI-HRMS $[M+H]^+$ calculated for $C_{25}H_{29}N_5O$: 416.24449, found: 416.24442 HPLC t_{ret} = 6.920 min

3-(3-(1-Cyclohexyl-1,6-dihydroimidazo[4,5-d]pyrrolo[2,3-b]pyridin-2-yl)phenyl)-N,N-dimethylpropanamide (16) was obtained from 22 mg **7** and 4 mg Pd/C in 2.5 ml THF / MeOH (4:1) following general procedure C with a reaction time of one hour at ambient temperature. Flash chromatography with DCM / MeOH (3 – 10 %). Yield: 21 mg (95 %) of **16** as white foam. ^{1}H NMR (200 MHz, $CDCl_3$) δ 10.69 (br s, 1H), 8.85 (s, 1H), 7.57 (s, 1H), 7.52 – 7.36 (m, 4H), 6.91 (d, *J* = 3.7 Hz, 1H), 4.62 – 4.42 (m, 1H), 3.14 – 3.03 (m, 2H), 2.97 (d, *J* = 2.5 Hz, 6H), 2.75 – 2.64 (m, 2H), 2.58 – 2.37 (m, 2H), 2.07 – 1.77 (m, 5H), 1.51 – 1.35 (m, 3H); ^{13}C NMR (50 MHz, $CDCl_3$) δ 172.0, 153.7, 143.4, 142.6, 135.4, 135.2, 134.4, 131.1, 130.4, 129.9, 129.0, 127.3, 123.4, 105.7, 101.6, 56.9, 37.3, 35.6, 35.1, 31.3, 31.0, 25.8, 25.0. ESI-HRMS $[M+H]^+$ calculated for $C_{25}H_{29}N_5O$: 416.24449, found: 416.24448 HPLC t_{ret} = 7.009 min

3-(5-(1-Cyclohexyl-1,6-dihydroimidazo[4,5-d]pyrrolo[2,3-b]pyridin-2-yl)furan-2-yl)-N,N-dimethylpropanamide (17) was obtained from 35 mg **8** and 8 mg Pd/C in 4 ml EtOAc / MeOH (3:1) following general procedure C with a reaction time of four hour at ambient temperature. Flash chromatography with DCM / MeOH (4 – 10 %). Yield: 21 mg (60 %) of **17** as white solid. ^{1}H NMR (200 MHz, $CDCl_3$) δ 11.83 (bs, 1H), 8.86 (s, 1H), 7.47 (d, *J* = 3.3 Hz, 1H), 6.92 – 6.80 (m, 2H), 6.28 (d, *J* = 3.3 Hz, 1H), 4.98 – 4.74 (m, 1H), 3.14 (t, *J* = 7.6 Hz, 2H), 2.98 (d, *J* = 6.2 Hz, 6H), 2.75 (t, *J* = 7.6 Hz, 2H), 2.58 – 2.32 (m, 2H), 2.14 – 1.80 (m, 5H), 1.64 – 1.37 (m, 3H); ^{13}C NMR (50 MHz, $CDCl_3$) δ 171.3, 157.5, 144.8, 143.8, 143.4, 136.3, 135.5, 133.9, 123.3, 113.9, 107.9, 105.3, 100.8, 57.0, 37.2, 35.6, 31.8, 30.8, 26.0, 25.1, 24.0. ESI-HRMS $[M+Na]^+$ calculated for $C_{23}H_{27}N_5O_2$: 428.20570, found: 428.20570 HPLC t_{ret} = 6.980 min

3-(4-(1-Cyclohexyl-1,6-dihydroimidazo[4,5-d]pyrrolo[2,3-b]pyridin-2-yl)phenyl)propanenitrile (18) was prepared from 48 mg **12** as solution in 1.5 ml DMF and 23 mg cyanuric chloride in 1 ml DMF following general procedure B with a reaction time of 2 hours at ambient temperature. Flash purification with EtOAc / MeOH (0 – 20 %). Yield: 27 mg (53 %) of **18** as white solid. ^{1}H NMR (200 MHz, DMSO) δ 11.95 (br s, 1H), 8.63 (s, 1H), 7.78 – 7.39 (m, 5H), 6.90 – 6.67 (m, 1H), 4.72 – 4.05 (m, 1H), 3.09 – 2.82 (m, 4H), 2.45 – 2.22 (m, 2H), 2.01 – 1.64 (m, 5H), 1.52 – 1.25 (m, 3H); ^{13}C NMR (50 MHz, DMSO) δ 151.4, 144.4, 140.5, 135.8, 134.8, 132.4, 129.6, 129.4, 128.8, 123.9, 120.2, 104.3, 100.0, 55.9, 30.3, 30.3, 25.2, 24.3, 17.8. ESI-HRMS $[M+H]^+$ calculated for $C_{23}H_{23}N_5$: 370.20262, found: 370.20293 HPLC t_{ret} = 7.335 min

3-(3-(1-Cyclohexyl-1,6-dihydroimidazo[4,5-d]pyrrolo[2,3-b]pyridin-2-yl)phenyl)propanenitrile (19) was prepared from 40 mg **13** as solution in 1 ml DMF and 19 mg cyanuric chloride in 1 ml DMF following general procedure B with a reaction time of 3 hours at

ambient temperature. Flash purification first with DCM / MeOH (4 – 10 %), then EtOAc / MeOH (0 – 20 %). Yield: 19 mg (50 %) of **19** as greenish solid. ^{1}H NMR (200 MHz, $CDCl_3$) δ 11.89 (br s, 1H), 8.89 (s, 1H), 7.62 (s, 1H), 7.58 – 7.38 (m, 4H), 6.89 (d, *J* = 3.4 Hz, 1H), 4.63 – 4.40 (m, 1H), 3.07 (t, *J* = 7.3 Hz, 2H), 2.71 (t, *J* = 7.3 Hz, 2H), 2.60 – 2.39 (m, 2H), 2.08 – 1.90 (m, 4H), 1.87 – 1.76 (m, 1H), 1.55 – 1.35 (m, 3H); ^{13}C NMR (50 MHz, $CDCl_3$) δ 152.4, 144.8, 138.9, 136.2, 135.5, 133.8, 131.9, 129.9, 129.8, 129.3, 128.4, 123.3, 119.0, 105.4, 101.1, 56.8, 31.6, 31.0, 25.7, 24.9, 19.3. ESI-HRMS $[M+H]^+$ calculated for $C_{23}H_{23}N_5$: 370.20262, found: 370.20270 HPLC t_{ret} = 7.467 min

3-(5-(1-Cyclohexyl-1,6-dihydroimidazo[4,5-d]pyrrolo[2,3-b]pyridin-2-yl)furan-2-yl)propanenitrile (20) was prepared from 40 mg **14** as solution in 1 ml DMF and 20 mg cyanuric chloride in 1 ml DMF following general procedure B with a reaction time of one hour at ambient temperature. Flash purification with EtOAc / MeOH (0 – 20 %). Yield: 25 mg (66 %) of **20** as off-white solid. ^{1}H NMR (200 MHz, DMSO) δ 11.98 (br s, 1H), 8.62 (s, 1H), 7.59 – 7.44 (m, 1H), 7.03 (d, *J* = 3.2 Hz, 1H), 6.84 – 6.74 (m, 1H), 6.56 (d, *J* = 3.2 Hz, 1H), 4.92 – 4.67 (m, 1H), 3.12 (t, *J* = 6.7 Hz, 2H), 2.94 (t, *J* = 6.7 Hz, 2H), 2.44 – 2.19 (m, 2H), 2.03 – 1.69 (m, 5H), 1.63 – 1.39 (m, 3H); ^{13}C NMR (50 MHz, DMSO) δ 154.3, 144.6, 143.7, 142.0, 135.9, 134.7, 132.5, 124.0, 119.8, 113.8, 108.9, 104.2, 99.8, 56.1, 30.3, 25.2, 24.4, 23.6, 15.6. ESI-HRMS $[M+H]^+$ calculated for $C_{21}H_{21}N_5O$: 360.18189, found: 360.18214 HPLC t_{ret} = 7.180 min

General Procedure D for Knoevenagel condensation to Cyanoacrylamides (21-28). Aldehyde **41**, **42** or **43** and corresponding cyanoacetamide or malononitrile (1.1 to 1.5 eq) were dissolved in alcoholic solvent (MeOH, EtOH or iPrOH). Piperidine (0.1 eq) was added to the stirred solution and the mixture was heated to 60-80 °C or ambient temperature until TLC or HPLC indicated complete conversion. The products were either isolated by filtration or flash

purification. The compounds were usually isolated as mixture of E/Z isomers, resulting in NMR spectra of high complexity.

(E/Z)-2-Cyano-3-(4-(1-cyclohexyl-1,6-dihydroimidazo[4,5-d]pyrrolo[2,3-b]pyridin-2-yl)phenyl)-N,N-dimethylacrylamide (21) was prepared from 51 mg **41** and 25 mg 2-cyano-N,N-dimethylacetamide (1.5 eq) in 2 ml EtOH following general procedure D at 70° C heating block temperature. The solvents were evaporated and the residue subjected to flash chromatography (DCM / MeOH 1-7%). Yield: 26 mg (41%) as yellow solid. ^{1}H NMR (400 MHz, $CDCl_3$) δ 11.81 (br s, 1H), 9.06 – 8.81 (m, 1H), 8.07 (d, *J* = 8.3 Hz) and 7.73 (d, *J* = 8.3 Hz, 2H), 7.84 (s) and 7.40 (s, 1H), 7.81 (d, *J* = 8.3 Hz) and 7.60 (d, *J* = 8.3 Hz, 1H), 7.51 (d, *J* = 3.3 Hz, 1H), 6.90 (d, *J* = 3.3 Hz, 1H), 4.61 – 4.37 (m, 1H), 3.34 – 2.97 (m, 6H), 2.63 – 2.43 (m, 2H), 2.09 – 1.77 (m, 5H), 1.59 – 1.34 (m, 3H). ^{13}C NMR (100 MHz, $CDCl_3$) δ 163.7, 162.3, 151.5, 151.4, 150.9, 145.5, 144.8, 136.6, 135.7, 134.8, 134.1, 134.1, 134.0, 133.6, 133.4, 130.5, 130.4, 130.3, 129.6, 123.4, 115.9, 108.0, 105.4, 101.2, 101.2, 57.1, 39.2, 37.9, 36.6, 35.3, 31.1, 25.8, 24.9. ESI-HRMS $[M+H]^+$ calculated for $C_{26}H_{26}N_6O$: 439.22409, found: 439.22423 HPLC t_{ret} = 6.457 min and 7.190 min (E/Z mixture)

(E/Z)-2-Cyano-3-(3-(1-cyclohexyl-1,6-dihydroimidazo[4,5-d]pyrrolo[2,3-b]pyridin-2-yl)phenyl)-N,N-dimethylacrylamide (22) was prepared from 51 mg **42** and 25 mg 2-cyano-N,N-dimethylacetamide (1.5 eq) in 2 ml EtOH following general procedure D at 70° C heating block temperature. The solvents were evaporated and the residue subjected to flash chromatography (DCM / MeOH 1-7%). Yield: 13 mg (20%) as yellow solid. ^{1}H NMR (200 MHz, $CDCl_3$) δ 11.59 (br s, 1H), 8.87 (s, 1H), 8.13 (s, 1H), 7.87 – 7.74 (m, 2H), 8.09 (s) and 7.72 – 7.58 (m, 2H), 7.50 (d, *J* = 3.1 Hz, 1H), 6.96 – 6.83 (m, 1H), 4.57 – 4.33 (m, 1H), 3.30 – 3.00 (m, 6H), 2.62 – 2.35 (m, 2H), 2.09 – 1.78 (m, 5H), 1.55 – 1.36 (m, 3H). ESI-HRMS

$[M+H]^+$ calculated for $C_{26}H_{26}N_6O$: 439.22409, found: 439.22417 HPLC t_{ret} = 6.797 min and 7.680 min (E/Z mixture)

(E/Z)-2-Cyano-3-(5-(1-cyclohexyl-1,6-dihydroimidazo[4,5-d]pyrrolo[2,3-b]pyridin-2-yl)furan-2-yl)-N,N-dimethylacrylamide (23) was prepared from 669 mg **43** and 247 mg 2-cyano-N,N-dimethylacetamide (1.1 eq) in 10 ml MeOH following general procedure D at 60° C oil-bath temperature. After complete conversion (ca. 90 min) the reaction mixture was cooled to -20 °C for several hours. The precipitate was collected by filtration and was washed with cold MeOH yielding the title compound with no need of purification. Yield: 755 mg (88%) as yellow solid. ^{1}H NMR (400 MHz, DMSO) δ 12.05 (br s, 1H), 8.72 – 8.63 (m, 1H), 7.78 (s, 1H), 7.56 (s, 1H), 7.49 (d, J = 3.5 Hz, 1H), 7.39 (d, J = 3.5 Hz, 1H), 6.86 – 6.78 (m, 1H), 4.99 – 4.86 (m, 1H), 3.21 – 2.87 (m, 6H), 2.42 – 2.27 (m, 2H), 2.02 (d, J = 10.7 Hz, 2H), 1.95 – 1.84 (m, 2H), 1.80 – 1.70 (m, 1H), 1.66 – 1.42 (m, 3H). ^{13}C NMR (100 MHz, DMSO) δ 162.8, 149.5, 148.4, 144.6, 140.5, 136.3, 135.4, 135.1, 132.8, 124.1, 121.9, 116.3, 115.9, 104.1, 101.9, 100.3, 56.1, 30.4, 30.0, 24.9, 24.3 ESI-HRMS $[M+H]^+$ calculated for $C_{24}H_{24}N_6O_2$: 429.20335, found: 429.20357 HPLC t_{ret} = 6.172 min and 6.985 min (E/Z mixture).

(E/Z)-2-Cyano-3-(5-(1-cyclohexyl-1,6-dihydroimidazo[4,5-d]pyrrolo[2,3-b]pyridin-2-yl)furan-2-yl)-N-methylacrylamide (24) was prepared from 50 mg **43** and 18 mg **44** (1.2 eq, for preparation see Supporting Information) in 2 ml MeOH following general procedure D at 60° C heating block temperature. After complete conversion (2 hours) the reaction mixture was cooled to -20 °C for several hours. The precipitate was collected by filtration and was washed with cold MeOH yielding the title compound with no need of purification. Yield: 54 mg (87%) as yellow solid. ^{1}H NMR (400 MHz, DMSO) δ 12.10 (br s, 1H), 8.69 (s, 1H), 8.44 – 8.31 (m, 1H), 8.08 (s, 1H), 7.60 (d, J = 3.7 Hz, 1H), 7.59 – 7.53 (m, 1H), 7.42 (d, J = 3.7 Hz, 1H), 6.89 – 6.79 (m, 1H),

5.03 – 4.89 (m, 1H), 2.77 (d, J = 4.3 Hz, 3H), 2.44 – 2.29 (m, 2H), 2.09 – 1.98 (m, 2H), 1.96 – 1.85 (m, 2H), 1.80 – 1.71 (m, 1H), 1.69 – 1.42 (m, 3H). ^{13}C NMR (100 MHz, DMSO) δ 160.9, 149.5, 149.0, 144.7, 140.5, 136.3, 135.1, 135.1, 132.8, 124.1, 123.1, 116.5, 116.0, 104.1, 101.4, 100.4, 56.1, 30.0, 26.8, 24.9, 24.2. ESI-HRMS $[M+H]^+$ calculated for $C_{23}H_{22}N_6O_2$: 415.18770, found: 415.18817 HPLC t_{ret} = 6.796 min and 7.573 min (E/Z mixture)

2-(4-(1-Cyclohexyl-1,6-dihydroimidazo[4,5-d]pyrrolo[2,3-b]pyridin-2-yl)benzylidene)malononitrile (25) was prepared from 25 mg **41** and 6 mg malononitrile (1.2 eq) in 4 ml *i*PrOH following general procedure D at ambient temperature for six hours. The reaction was quenched with sat. NH_4Cl followed by extractive workup (5x10ml EtOAc). The combined organic extracts were dried over Na_2SO_4, evaporated and the residue subjected to flash chromatography (DCM / MeOH 4-10%). Yield: 18 mg (63%) as amorphous yellow solid. ^{1}H NMR (200 MHz, DMSO) δ 12.00 (bs, 1H), 8.77 – 8.50 (m, 2H), 8.13 (d, *J* = 6.9 Hz, 2H), 7.93 (d, *J* = 6.9 Hz, 2H), 7.56 – 7.45 (m, 1H), 6.86 – 6.70 (m, 1H), 4.49 – 4.23 (m, 1H), 2.41 – 2.20 (m, 2H), 2.05 – 1.75 (m, 5H), 1.48 – 1.24 (m, 3H). ^{13}C NMR (50 MHz, $CDCl_3$) δ 160.6, 150.1, 144.5, 136.1, 136.0, 135.0, 132.7, 132.0, 130.8, 130.5, 124.1, 114.2, 113.2, 104.3, 100.2, 82.48, 56.3, 30.2, 25.1, 24.3. ESI-HRMS $[M+H]^+$ calculated for $C_{24}H_{20}N_6$: 393.18222, found: 393.18275 HPLC t_{ret} = 7.826 min

2-(3-(1-Cyclohexyl-1,6-dihydroimidazo[4,5-d]pyrrolo[2,3-b]pyridin-2-yl)benzylidene)malononitrile (26) was prepared from 25 mg **42** and 6 mg malononitrile (1.2 eq) in 2 ml *i*PrOH following general procedure D at ambient temperature for six hours. The reaction was quenched with sat. NH_4Cl followed by extractive workup (5x10ml EtOAc). The combined organic extracts were dried over Na_2SO_4, evaporated and the residue subjected to flash chromatography (DCM / MeOH 4-10%). Yield: 16 mg (56%) as yellow solid. ^{1}H NMR (400

MHz, DMSO) δ 11.99 (bs, 1H), 8.70 (s, 1H), 8.67 (s, 1H), 8.21 (s, 1H), 8.17 (d, *J* = 7.6 Hz, 1H), 7.99 (d, *J* = 7.6 Hz, 1H), 7.85 (t, *J* = 7.6 Hz, 1H), 7.55 (s, 1H), 6.81 (s, 1H), 4.45 – 4.31 (m, 1H), 2.43 – 2.29 (m, 2H), 2.02 – 1.83 (m, 4H), 1.76 – 1.65 (m, 1H), 1.49 – 1.32 (m, 3H). ^{13}C NMR (100 MHz, DMSO) δ 160.8, 149.9, 144.5, 135.9, 134.9, 134.8, 132.4, 132.2, 131.7, 131.4, 131.0, 130.0, 124.0 114.0, 113.0, 104.2, 100.0, 82.8, 56.1, 30.3, 25.0, 24.2. ESI-HRMS $[M+H]^+$ calculated for $C_{24}H_{20}N_6$: 393.18222, found: 393.18238 HPLC t_{ret} = 8.393 min

2-((5-(1-Cyclohexyl-1,6-dihydroimidazo[4,5-d]pyrrolo[2,3-b]pyridin-2-yl)furan-2-yl)methylene)malononitrile (27) was prepared from 25 mg **43** and 7 mg malononitrile (1.2 eq) in 2 ml *i*PrOH following general procedure D at ambient temperature for one hour. The reaction was quenched with sat. NH_4Cl followed by extractive workup (5x10ml DCM). The combined organic extracts were dried over Na_2SO_4, evaporated and the residue subjected to flash chromatography (DCM / MeOH 4-10%). Yield: 32 mg (93%) as red solid. ^{1}H NMR (200 MHz, DMSO) δ 12.13 (bs, 1H), 8.70 (s, 1H), 8.40 (s, 1H), 7.66 (d, *J* = 3.8 Hz, 1H), 7.62 – 7.53 (m, 1H), 7.49 (d, *J* = 3.8 Hz, 1H), 6.83 (s, 1H), 5.08 – 4.81 (m, 1H), 2.45 – 2.20 (m, 2H), 2.10 – 1.83 (m, 4H), 1.80 – 1.43 (m, 4H). ^{13}C NMR (50 MHz, DMSO) δ 151.2, 149.0, 144.7, 143.8, 139.9, 136.6, 135.3, 133.0, 127.0, 124.2, 117.3, 114.6, 113.3, 104.1, 100.7, 75.5, 56.1, 29.9, 24.8, 24.2. ESI-HRMS $[M+H]^+$ calculated for $C_{22}H_{18}N_6O$: 383.16149, found: 383.16200 HPLC t_{ret} = 8.622 min

(E/Z)-3-(5-(1-Cyclohexyl-1,6-dihydroimidazo[4,5-d]pyrrolo[2,3-b]pyridin-2-yl)furan-2-yl)-2-(4-methylpiperazine-1-carbonyl)acrylonitrile (28) was prepared from 50 mg **43** and 30 mg **45** (1.2 eq, for preparation see Supporting Information) in 3 ml EtOH following general procedure D at 80° C heating block temperature. The solvents were evaporated and the residue subjected to flash chromatography (DCM / 0.5 M NH_3 in MeOH 5-10%). Yield: 59 mg (81%) as

orange solid. ^{1}H NMR (400 MHz, DMSO) δ 12.06 (br s, 1H), 8.76 – 8.59 (m, 1H), 7.76 (s) and 7.67 (s, 1H), 7.59 – 7.53 (m, 1H), 7.49 (d, *J* = 3.2 Hz) and 7.25 (d, *J* = 3.2 Hz, 1H), 7.39 (d, *J* = 3.2) and 7.21 (d, *J* = 3.2 Hz, 1H), 6.88 – 6.74 (m, 1H), 5.02 – 4.85 (m) and 4.70 – 4.57 (m, 1H), 3.45 – 3.24 (m, 4H), 2.40 – 2.24 (m, 5H), 2.22 – 2.16 (m, 3H), 2.08 – 1.83 (m, 5H), 1.81 – 1.68 (m, 1H), 1.66 – 1.42 (m, 3H). ^{13}C NMR (100 MHz, DMSO) δ 161.8, 159.9, 149.5, 149.1, 148.4, 147.7, 144.6, 140.4, 136.2, 136.2, 135.4, 135.0, 134.8, 132.7, 131.6, 124.0, 121.8, 120.3, 117.0, 116.2, 115.8, 115.7, 104.1, 104.0, 103.7, 101.5, 100.2, 99.9, 56.2, 56.0, 54.2, 54.1, 53.9, 53.8, 53.1, 45.9, 45.3, 45.1, 45.0, 41.5, 41.2, 30.2, 29.9, 24.9, 24.8, 24.5, 24.2. ESI-HRMS $[M+H]^+$ calculated for $C_{27}H_{29}N_7O_2$: 484.24555, found: 484.24556 HPLC t_{ret} = 4.632 min and 5.008 min (E/Z mixture)

Synthesis of *N*^{4}-Cyclohexyl-1-tosyl-1*H*-pyrrolo[2,3-*b*]pyridine-4,5-diamine (34). *Step 1: 4-Chloro-1-tosyl-1H-pyrrolo[2,3-b]pyridine (**31**).* In a 500 ml round bottomed flask 9.77 g 4-Chloro-7-Azaindole (64 mmol, 1.0 eq) were dissolved in 280 ml dry THF and the solution was cooled with ice / water. To the stirred solution were added 3.07 g NaH (60% disp. In mineral oil, 76.8 mmol, 1.2 eq) portion wise. After complete addition stirring was continued for 15 min followed by the dropwise addition of 12.82 g tosyl chloride (67.2 mmol, 1.05 eq) as solution in 40 ml dry THF. The cooling bath was removed after complete addition and the reaction mixture was stirred for 2 hours at ambient temperature. At this point HPLC indicated full consumption of starting material. The reaction was quenched by careful addition of 10 ml saturated NH_4Cl solution. The mixture was diluted with EtOAc and transferred to a separatory funnel. The organic phase was washed twice with 100 ml 1M K_2CO_3 and once with brine. The organic phase was dried over Na_2SO_4 and evaporated under reduced pressure. The resulting solid was triturated with cold MeOH and the solvent was decanted off yielding 18.32 g (93 %) of the title compound

as brown solid. ^{1}H NMR (200 MHz, $CDCl_3$) δ 8.30 (d, J = 5.3 Hz, 1H), 8.06 (d, J = 8.4 Hz, 2H), 7.76 (d, J = 4.0 Hz, 1H), 7.27 (d, J = 8.4 Hz, 2H), 7.18 (d, J = 5.3 Hz, 1H), 6.68 (d, J = 4.0 Hz, 1H), 2.36 (s, 3H); ^{13}C NMR (50 MHz, $CDCl_3$) δ 147.6 145.6, 145.4, 136.8, 135.2, 129.8, 128.2, 127.0, 122.3, 119.1, 103.4, 21.7. DC-MS (ESI) m/z: 305.2 $[M-H]^-$ HPLC t_{ret} = 8.47 min.

*Step 2: 4-Chloro-5-nitro-1-tosyl-1H-pyrrolo[2,3-b]pyridine (**32**).* In a 500 ml three-necked round bottomed flask were dissolved 18.30 g **31** (59.6 mmol, 1.0 eq) and 10.55 g tetramethylammonium nitrate (77.5 mmol, 1.3 eq) in 300 ml dry DCM and the solution was cooled with ice / water to an internal temperature of 0-5 °C. To the stirred solution were slowly added 16.28 g trifluoroacetic anhydride (77.5 mmol, 1.3 eq) via syringe pump over the course of ten hours. After complete addition the mixture was allowed to reach ambient temperature slowly and stirring was continued overnight. HPLC indicated full conversion and the reaction was diluted with DCM up to a total volume of ca. 500 ml. The organic phase was successively washed with water, sat. $NaHCO_3$, sat. Na_2CO_3 and brine. The organic phase was dried over Na_2SO_4 and concentrated under reduced pressure almost to dryness. The yellow suspension was taken up in a small amount of MeOH and stored at -20 °C for several hours. The solids were isolated by filtration, washed sparingly with cold MeOH and dried in vacuo to yield 14.14 g (67 %) of the title compound as beige fine needles. ^{1}H NMR (200 MHz, $CDCl_3$) δ 8.99 (s, 1H), 8.07 (d, *J* = 8.4 Hz, 2H), 7.93 (d, *J* = 4.1 Hz, 1H), 7.32 (d, *J* = 8.4 Hz, 2H), 6.85 (d, *J* = 4.0 Hz, 1H), 2.40 (s, 3H); ^{13}C NMR (50 MHz, $CDCl_3$) δ 147.2, 146.6, 142.3, 140.6, 134.4, 131.3, 130.1, 130.0, 128.6, 123,0, 104.5, 21.9. DC-MS (ESI) m/z: 406.0 $[M+Na+MeOH]^+$ HPLC t_{ret} = 8.82 min.

*Step 3: N-Cyclohexyl-5-nitro-1-tosyl-1H-pyrrolo[2,3-b]pyridin-4-amine (**33**).* In a 1L round bottomed flask 14.10 g **32** (40 mmol, 1.0 eq) were suspended in 180 ml *i*PrOH. To the stirred

suspension was added a mixture 7.9 ml Et_3N (56 mmol, 1.4 eq) and 5.7 ml cyclohexylamine (50 mmol, 1.25 eq) at ambient temperature. The mixture was heated to reflux for 60 min. At this point reaction control (HPLC) indicated full consumption of starting material. A mixture of 360 ml H_2O and 180 ml sat. NH_4Cl solution was added slowly to the hot reaction mixture causing the precipitation of solids. After complete addition the suspension was stirred for 5 min at elevated temperature and was then cooled down in an ice bath under moderate stirring for another 30 min. The solids were collected by filtration, washed with water and dried in vacuo affording 15.55 g (94 %) of the title compound as an orange to red granular solid, which was carried on to the next step without further purification. ^{1}H NMR (200 MHz, $CDCl_3$) δ 9.20 – 8.95 (m, 2H), 8.05 (d, *J* = 8.4 Hz, 2H), 7.57 (d, *J* = 4.1 Hz, 1H), 7.29 (d, *J* = 8.4 Hz, 2H), 6.69 (d, *J* = 4.1 Hz, 1H), 3.94 (m, 1H), 2.38 (s, 3H), 2.19 – 1.99 (m, 2H), 1.93 – 1.58 (m, 3H), 1.57 – 1.31 (m, 5H); ^{13}C NMR (50 MHz, $CDCl_3$) δ 146.41, 145.9, 144.9, 134.9, 129.8, 128.6, 126.6, 123.6, 107.6, 106.7, 52.9, 33.5, 25.4, 24.4, 21.8. DC-MS (ESI) m/z: 469.5 $[M+Na+MeOH]^+$ HPLC t_{ret} = 10.17 min.

*Step 4: N^4-Cyclohexyl-1-tosyl-1H-pyrrolo[2,3-b]pyridine-4,5-diamine (**34**).* In a 1L two-necked round-bottomed flask 15.52 g **33** (40.4 mmol) were suspended in a mixture of 120 ml MeOH and 360 ml EtOAc. The stirred mixture was purged with nitrogen for 5 min, then 750 mg Pd/C were added. Subsequently the mixture was purged with hydrogen for 10 min, then the flask was sealed with a rubber septum and a hydrogen reservoir was attached via cannula. The reaction mixture was heated up to 60 °C oil-bath temperature and stirred for about 36 hours until TLC indicated full consumption of starting material. The catalyst was removed by filtration over a celite pad and was washed thoroughly with MeOH and EtOAc. The filtrate darkened rapidly during filtration upon contact to air oxygen. It was concentrated under reduced pressure and co-

evaporated with DCM to yield 14.40 g **34** (quant.) as purple foam. The vicinal diamine **34** seems not to be suitable for long term storage under shelf conditions and should be carried on to the next step as soon as possible. ^{1}H NMR (200 MHz, $CDCl_3$) δ 7.99 (d, *J* = 8.1 Hz, 2H), 7.82 (s, 1H), 7.44 (d, *J* = 4.1 Hz, 1H), 7.21 (d, *J* = 8.1 Hz, 2H), 6.53 (d, *J* = 4.1 Hz, 1H), 4.75 (bs, 1H), 3.77 – 3.57 (m, 1H), 2.96 (bs, 2H), 2.33 (s, 3H), 2.11 – 1.95 (m, 2H), 1.86 – 1.57 (m, 3H), 1.45 – 1.10 (m, 5H); ^{13}C NMR (50 MHz, $CDCl_3$) δ 145.8, 144.8, 141.0, 137.1, 135.7, 129.6, 128.0, 123.1, 122.3, 108.0, 105.0, 52.5, 34.4, 25.7, 2.9, 21.7. DC-MS (ESI) m/z: 385.4 $[M+H]^+$ HPLC t_{ret} = 6.97 min.

General Procedure E for Imidazole Ring Closure. A solution of **34** (1 eq) and corresponding aldehyde (1.2 eq) in DMF (0.2 M) was stirred for 15 min at ambient temperature. Then 3 % v/v water and $KHSO_5$ (0.7 eq) were added and stirring was continued until TLC indicated complete conversion. The reaction mixture was poured in 0.2 M K_2CO_3 solution (2 eq), the precipitate filtered off, dried in vacuo and purified by column chromatography unless otherwise stated.

(4-(1-Cyclohexyl-6-tosyl-1,6-dihydroimidazo[4,5-d]pyrrolo[2,3-b]pyridin-2-yl)phenyl)methanol (35) was obtained from 384 mg **34** and 164 mg 4-(hydroxymethyl)benzaldehyde following general procedure E with a reaction time of two hours at ambient temperature. Crude product afforded flash purification using gradient elution (petrol ether / (EtOAc+5% MeOH) 50 – 100%) to yield 343 mg (69 %) of **35** as brownish foam. ^{1}H NMR (200 MHz, $CDCl_3$) δ 8.94 (s, 1H), 8.10 (d, *J* = 8.4 Hz, 2H), 7.83 (d, *J* = 4.1 Hz, 1H), 7.44 (q, *J* = 8.5 Hz, 4H), 7.25 (d, *J* = 8.4 Hz, 2H), 6.97 (d, *J* = 4.1 Hz, 1H), 4.77 (s, 2H), 4.40 (tt, *J* = 12.1, 3.8 Hz, 1H), 3.76 (br s, 1H), 2.40 – 2.14 (m, 5H), 2.00 – 1.71 (m, 5H), 1.47 – 1.28 (m, 3H). ^{13}C NMR (50 MHz, $CDCl_3$) δ 154.0, 145.3, 144.0, 142.9, 138.3, 137.0, 135.4, 133.0, 129.7,

129.5, 129.1, 128.4, 126.9, 124.7, 107.8, 105.1, 64.2, 56.8, 31.1, 25.6, 24.9, 21.7 DC-MS (ESI) m/z: 522.9 $[M+Na]^+$ HPLC t_{ret} = 8.077 min.

(3-(1-Cyclohexyl-6-tosyl-1,6-dihydroimidazo[4,5-d]pyrrolo[2,3-b]pyridin-2-yl)phenyl)methanol (36) was obtained from 264 mg **34** and 112 mg 3-(hydroxymethyl)benzaldehyde following general procedure E with a reaction time of one hour at ambient temperature. Crude product afforded flash purification using gradient elution (petrol ether / (EtOAc+5% MeOH) 30 – 100%) to yield 247 mg (72 %) of **36** as brownish foam. ^{1}H NMR (200 MHz, $CDCl_3$) δ 8.93 (s, 1H), 8.11 (d, *J* = 8.3 Hz, 2H), 7.85 (d, *J* = 4.1 Hz, 1H), 7.62 (s, 1H), 7.53 – 7.39 (m, 3H), 7.26 (d, *J* = 8.3 Hz, 3H), 6.97 (d, *J* = 4.1 Hz, 1H), 4.75 (s, 2H), 4.56 – 4.30 (m, 1H), 2.95 (bs, 1H), 2.40 – 2.12 (m, 5H), 2.04 – 1.72 (m, 5H), 1.46 – 1.29 (m, 3H). ^{13}C NMR (50 MHz, $CDCl_3$) δ 153.9, 145.3, 142.9, 142.5, 138.2, 136.6, 135.4, 132.9, 130.3, 129.7, 128.9, 128.7, 128.4, 128.3, 128.1, 124.9, 107.8, 105.0, 64.5, 56.9, 31.1, 25.6, 24.9, 21.8 FAB-MS m/z: 501.2 $[M+H]^+$ HPLC t_{ret} = 8.333 min.

(5-(1-Cyclohexyl-6-tosyl-1,6-dihydroimidazo[4,5-d]pyrrolo[2,3-b]pyridin-2-yl)furan-2-yl)methanol (37) was obtained from 14.5 g **34** and 5.7 g 5-(hydroxymethyl)furfural following general procedure E with a reaction time of 2 hours at ambient temperature. The crude product (ca. 17 g) was redissolved in DCM / MeOH, 34 g Celite were added and the solvents were stripped off again. The solids were loaded on a short plug of silica (10 cm diameter, 3 cm height) and covered with wool. The short column was conditioned with petrol ether followed by elution with 2000 ml EtOAc + 5% MeOH. The filtrate was concentrated to a thick brown oil and was taken up in a minimal amount of warm MeOH. The dark solution was diluted with the approximately same volume of Et_2O and cooled for several hours in an ice-bath. The formed precipitate was isolated by filtration, washed with Et_2O and dried in vacuo (10.5g). For a second

crop, the mother liquor and washings were evaporated and subjected to flash chromatography (petrol ether / (EtOAc+5% MeOH) 50 – 100%) to yield another 2 grams. Total yield: 12.5 g (68 %) of **37** as pale brownish solid. ^{1}H NMR (200 MHz, $CDCl_3$) δ 8.89 (s, 1H), 8.10 (d, *J* = 8.4 Hz, 2H), 7.83 (d, *J* = 4.1 Hz, 1H), 7.25 (d, *J* = 8.4 Hz, 2H), 6.92 (d, *J* = 4.1 Hz, 1H), 6.89 (d, *J* = 3.4 Hz, 1H), 6.44 (d, *J* = 3.4 Hz, 1H), 4.85 – 4.61 (m, 3H), 2.33 (s, 3H), 2.28 – 2.08 (m, 2H), 1.95 – 1.72 (m, 5H), 1.45 – 1.27 (m, 3H) ^{13}C NMR (50 MHz, $CDCl_3$) δ 156.9, 145.3, 144.4, 143.6, 142.9, 138.3, 136.9, 135.4, 133.2, 129.7, 128.4, 124.8, 114.5, 109.8, 107.8, 104.7, 57.4, 57.3, 30.8, 25.8, 24.9, 21.7 DC-MS (ESI) m/z: 491.3 $[M+H]^+$ HPLC t_{ret} = 8.112 min.

General Procedure F for Dess-Martin-Oxidation of Phenylmethanols 35 and 36. A ice-cooled solution of **35** or **36** in DCM (0.2 M) was treated with Dess-Martin-Periodinane (1.2 eq). After addition the mixture was allowed to warm up to ambient temperature and stirring was continued until TLC indicated complete conversion. Saturated $NaHCO_3$ solution was added and the biphasic mixture was transferred to a separatory funnel. The aqueous phase was extracted five times with DCM and the combined organics were dried over Na_2SO_4 and evaporated. The crude product was purified via flash chromatography.

4-(1-Cyclohexyl-6-tosyl-1,6-dihydroimidazo[4,5-d]pyrrolo[2,3-b]pyridin-2-yl)benzaldehyde (38) was obtained from 148 mg **35** following general procedure F. Flash purification with gradient (petrol ether / (EtOAc+5% MeOH) 30 – 80%). Yield 118 mg (80 %) of **38** as brownish foam. ^{1}H NMR (200 MHz, $CDCl_3$) δ 10.10 (s, 1H), 8.94 (s, 1H), 8.17 – 7.95 (m, 4H), 7.84 (d, *J* = 4.0 Hz, 1H), 7.79 (d, *J* = 7.8 Hz, 2H), 7.24 (d, *J* = 7.8 Hz, 2H), 6.97 (d, *J* = 4.0 Hz, 1H), 4.53 – 4.28 (m, 1H), 2.41 – 2.17 (m, 5H), 2.05 – 1.75 (m, 5H), 1.55 – 1.28 (m, 3H). ^{13}C NMR (50 MHz, $CDCl_3$) δ 191.6, 152.5, 145.3, 142.9, 138.8, 137.3, 137.2 136.4, 135.3,

133.2, 130.3, 130.0, 129.7, 128.3, 124.9, 107.8, 104.9, 57.1, 31.1, 25.6, 24.8, 21.7 DC-MS (ESI) m/z: 520.9 $[M+Na]^+$ HPLC t_{ret} = 8.347 min.

3-(1-Cyclohexyl-6-tosyl-1,6-dihydroimidazo[4,5-d]pyrrolo[2,3-b]pyridin-2-yl)benzaldehyde (39) was obtained from 240 mg **36** following general procedure F. Flash purification using gradient elution (petrol ether / (EtOAc+5% MeOH) 30 – 80%). Yield: 220 mg (92 %) of **39** as brownish foam. ^{1}H NMR (200 MHz, $CDCl_3$) δ 8.93 (s, 1H), 8.11 (d, *J* = 8.3 Hz, 2H), 7.85 (d, *J* = 4.1 Hz, 1H), 7.62 (s, 1H), 7.53 – 7.39 (m, 3H), 7.26 (d, *J* = 8.3 Hz, 3H), 6.97 (d, *J* = 4.1 Hz, 1H), 4.75 (s, 2H), 4.56 – 4.30 (m, 1H), 2.95 (bs, 1H), 2.40 – 2.12 (m, 5H), 2.04 – 1.72 (m, 5H), 1.46 – 1.29 (m, 3H). ^{13}C NMR (50 MHz, $CDCl_3$) δ 153.9, 145.3, 142.9, 142.5, 138.2, 136.6, 135.4, 132.9, 130.3, 129.7, 128.9, 128.7, 128.4, 128.3, 128.1, 124.9, 107.8, 105.0, 64.5, 56.9, 31.1, 25.6, 24.9, 21.8 FAB-MS m/z: 499.2 $[M+H]^+$ HPLC t_{ret} = 8.751 min.

5-(1-Cyclohexyl-6-tosyl-1,6-dihydroimidazo[4,5-d]pyrrolo[2,3-b]pyridin-2-yl)furan-2-carbaldehyde (40). 12.2 g (24.9 mmol, 1.0 eq) of **37** and 469 mg (1.25 mmol, 0.05 eq) $Cu(MeCN)_4 \cdot OTf$ were partially dissolved in 180 ml MeCN in a schlenk flask. TEMPO (1.25 mmol, 0.05 eq), 2,2´-bipyridine (1.25 mmol, 0.05 eq) and N-Methylimidazole (2.5 mmol, 0.1 eq) were added as solution in MeCN and the reaction mixture was stirred under a slightly positive pressure of oxygen overnight at 50 °C water-bath temperature. During the course of the reaction, starting material dissolves and the product precipitates partially. The mixture was cooled to 0-5 °C and the precipitate was collected by filtration. The filtrate was passed through a plug of silica and eluted with EtOAc. The volatiles were removed and the residue together with the filtered crude product were subjected to column chromatography (PE/EtOAC+5% MeOH 20->80%) to yield 10.5 g (87%) of **40** as yellow to orange solid. ^{1}H NMR (200 MHz, $CDCl_3$) δ 9.77 (s, 1H), 8.93 (s, 1H), 8.12 (d, *J* = 8.5 Hz, 2H), 7.86 (d, *J* = 4.1 Hz, 1H), 7.41 (d, *J* = 3.7 Hz, 1H), 7.32 –

7.22 (m, 3H), 6.98 (d, *J* = 4.1 Hz, 1H), 5.10 – 4.88 (m, *J* = 12.2 Hz, 1H), 2.43 – 2.20 (m, 5H), 2.11 – 1.84 (m, 5H), 1.63 – 1.43 (m, 3H). ^{13}C NMR (50 MHz, $CDCl_3$) δ 177.4, 153.2, 149.7, 145.4, 143.2, 142.6, 139.0, 137.4, 135.4, 133.8, 129.8, 128.4, 125.0, 122.0, 115.4, 107.8, 104.6, 57.9, 31.0, 26.0, 25.0, 21.8 DC-MS (ESI) m/z: 511.3 $[M+Na]^+$ HPLC t_{ret} = 8.520 min

General Procedure G for Tosyl Cleavage. Aldehyde **38**, **39** or **40** was suspended in a 1 M solution of KOH in MeOH and the mixture was stirred until TLC indicated complete consumption of starting material. The reaction was quenched by addition of sat. NH_4Cl followed by dilution with enough EtOAc and water to get clear phases. The organic phase was washed two times with water and once with brine and then dried over Na_2SO_4 and evaporated. The residue was subjected to column chromatography.

4-(1-Cyclohexyl-1,6-dihydroimidazo[4,5-d]pyrrolo[2,3-b]pyridin-2-yl)benzaldehyde (41) was obtained from 362 mg **38** following general procedure G. Flash purification with DCM / MeOH (3 – 10%). Yield: 188 mg (75 %) of **41** as off-white solid. ^{1}H NMR (200 MHz, DMSO) δ 12.03 (br s, 1H), 10.15 (s, 1H), 8.68 (s, 1H), 8.12 (d, *J* = 7.8 Hz, 2H), 7.93 (d, *J* = 7.8 Hz, 2H), 7.61 – 7.50 (m, 1H), 6.84 – 6.76 (m, 1H), 4.55 – 4.24 (m, 1H), 2.46 – 2.23 (m, 2H), 1.88 (dd, *J* = 35.2, 24.7 Hz, 5H), 1.52 – 1.22 (m, 3H). ^{13}C NMR (50 MHz, DMSO) δ 192.5, 150.1, 144.2, 136.2, 136.2, 135.8, 134.7, 132.3, 130.1, 129.4, 123.8, 104.1, 100.0, 56.1, 30.3, 25.1, 24.3 DC-MS (ESI) m/z: 342.9 $[M-H]^-$ HPLC t_{ret} = 6.975 min

3-(1-Cyclohexyl-1,6-dihydroimidazo[4,5-d]pyrrolo[2,3-b]pyridin-2-yl)benzaldehyde (42) was obtained from 340 mg **39** following general procedure G. Flash purification with DCM / MeOH (3 – 10%) to yield 178 mg (76 %) of **42** as beige solid. ^{1}H NMR (200 MHz, $CDCl_3$) δ 11.85 (br s, 1H), 10.13 (s, 1H), 8.91 (s, 1H), 8.21 (s, 1H), 8.07 (d, *J* = 7.6 Hz, 1H), 7.96 (d, *J* = 7.6 Hz, 1H), 7.74 (t, *J* = 7.6 Hz, 1H), 7.52 (d, *J* = 3.5 Hz, 1H), 6.90 (d, *J* = 3.5 Hz, 1H), 4.57 –

4.34 (m, 1H), 2.53 (dd, *J* = 23.9, 12.3 Hz, 2H), 2.12 – 1.76 (m, 5H), 1.59 – 1.31 (m, 3H). ^{13}C NMR (50 MHz, $CDCl_3$) δ 191.6, 151.4, 144.6, 136.9, 136.2, 135.5, 135.3, 134.0, 132.4, 131.1, 130.7, 129.7, 123.5, 105.5, 101.1, 57.2, 31.1, 25.8, 24.9 FAB-MS m/z: 345.2 $[M+H]^+$ HPLC t_{ret} = 6.152 min

5-(1-Cyclohexyl-1,6-dihydroimidazo[4,5-d]pyrrolo[2,3-b]pyridin-2-yl)furan-2-carbaldehyde (43) was obtained from 6.0 g **40** following general procedure G. Flash purification with DCM / MeOH (3 – 10%) to yield 2.24 g (54 %) of **43** as yellow solid. ^{1}H NMR (200 MHz, $CDCl_3$) δ 12.05 (br s, 1H), 9.78 (s, 1H), 8.89 (s, 1H), 7.51 (d, *J* = 3.4 Hz, 1H), 7.42 (d, *J* = 3.7 Hz, 1H), 7.30 (d, *J* = 3.7 Hz, 1H), 6.90 (d, *J* = 3.4 Hz, 1H), 5.17 – 4.94 (m, 1H), 2.63 – 2.36 (m, 2H), 2.18 – 1.79 (m, 5H), 1.69 – 1.43 (m, 3H). ^{13}C NMR (50 MHz, $CDCl_3$) δ 177.5, 153.1, 150.3, 145.1, 141.4, 136.8, 135.7, 134.4, 123.6, 122.0, 114.7, 105.2, 100.9, 57.8, 30.9, 26.0, 25.0 DC-MS (ESI) m/z: 357.2 $[M+Na]^+$ HPLC t_{ret} = 6.991 min

ASSOCIATED CONTENT

Supporting Information.

The Supporting Information is available free of charge on the ACS Publications website at DOI: xxx

SMILES codes of final compounds (CSV).

Additional experimental procedures and data for the preparation of intermediates and compound **29** and **30**; X-ray crystallographic diffraction data (PDF).

Kinome selectivity data for compound **23** (PDF).

Accession Codes.

Cocrystal structures of JAK3 in complex with compounds **10**, **11** and **20** are deposited in the Protein Data Bank under the accession codes JAK3-10, JAK3-11 and JAK3-20, respectively. The authors will release the atomic coordinates and experimental data upon article publication.

AUTHOR INFORMATION

Corresponding Author

*Phone: +49 7071 2972459. E-mail: stefan.laufer@uni-tuebingen.de

Author Contributions

The manuscript was written through contributions of all authors. All authors have given approval to the final version of the manuscript.

Notes

The authors declare no competing financial interests.

ACKNOWLEDGMENT

S.K. and A.C. are grateful for financial support by the DFG Sonderforschungsbereich SFB1177 Autophagy. K.G. and J.H. are supported by the DFG FOR 2497/TP02 (GH133/2-1). S.K., A.C., S.M. and B.T. would like to acknowledge support by the SGC, a registered charity (number 1097737) that receives funds from AbbVie, Bayer Pharma AG, Boehringer Ingelheim, Canada Foundation for Innovation, Eshelman Institute for Innovation, Genome Canada through Ontario Genomics Institute, Innovative Medicines Initiative (EU/EFPIA) [ULTRA-DD grant no. 115766], Janssen, Merck & Co., Novartis Pharma AG, Ontario Ministry of Economic Development and Innovation, Pfizer, São Paulo Research Foundation-FAPESP, and Takeda and the Centre of Excellence Macromolecular complexes (CEF) at Frankfurt University. S.K. and

S.L are grateful for support by the German Cancer network DKTK. M.G. gratefully acknowledges funding by the Recruitment of Excellent Junior Researchers Grant of the University of Tübingen.

M.F., M.G. and T.D. thank Silke Bauer, Katharina Bauer and Daniela Müller for biological testing of the final compounds.

ABBREVIATIONS

bpy, 2,2'-bipyridyl; BRET, bioluminescence resonance energy transfer; DBU, 1,8-Diazabicyclo[5.4.0]undec-7-ene; DCM, dichloromethane; DMF, *N,N*-dimethylformamide; DMP, Dess-Martin periodinane; DTT, dithiothreitol; HWE, Horner-Wadsworth-Emmons; IC_{50}, half maximal inhibitory concentration; IFN, interferon; IL, interleukin; JAK, janus kinase; NMI, *N*-methylimidazole; PBMC, peripheral blood mononuclear cells; SAR, structure activity relationship; SCID, severe combined immunodeficiency; STAT, signal transducer and activator of transcription; TEMPO, 2,2,6,6-Tetramethylpiperidinyloxyl; TFAA, trifluoroacetic anhydride; TYK2, tyrosine kinase 2

REFERENCES.

1. Villarino, A. V.; Kanno, Y.; O'Shea, J. J. Mechanisms and consequences of JAK-STAT signaling in the immune system. *Nature Immunology* **2017,** *18* (4), 374-384.

2. Leonard, W. J.; O'Shea, J. J. JAKs and STATs: biological implications. *Annual Review of Immunology* **1998,** *16* (1), 293-322.

3. Rochman, Y.; Spolski, R.; Leonard, W. J. New insights into the regulation of T cells by γc family cytokines. *Nature Reviews Immunology* **2009,** *9* (7), 480-490.

4. Ghoreschi, K.; Laurence, A.; O'Shea, J. J. Janus kinases in immune cell signaling. *Immunological Reviews* **2009,** *228* (1), 273-287.

5. Pesu, M.; Candotti, F.; Husa, M.; Hofmann, S. R.; Notarangelo, L. D.; O'Shea, J. J. JAK3, severe combined immunodeficiency, and a new class of immunosuppressive drugs. *Immunological Reviews* **2005,** *203* (1), 127-142.

6. O'Shea, J. J.; Pesu, M.; Borie, D. C.; Changelian, P. S. A new modality for immunosuppression: targeting the JAK/STAT pathway. *Nature Reviews Drug Discovery* **2004,** *3* (7), 555-564.

7. Schwartz, D. M.; Kanno, Y.; Villarino, A.; Ward, M.; Gadina, M.; O'Shea, J. J. JAK inhibition as a therapeutic strategy for immune and inflammatory diseases. *Nature Reviews Drug Discovery* **2017,** *16*, 843.

8. Ghoreschi, K.; Laurence, A.; O'Shea, J. J. Selectivity and therapeutic inhibition of kinases: to be or not to be? *Nature Immunology* **2009,** *10*, 356-360.

9. Haan, C.; Rolvering, C.; Raulf, F.; Kapp, M.; Drückes, P.; Thoma, G.; Behrmann, I.; Zerwes, H.-G. JAK1 has a dominant role over JAK3 in signal transduction through gamma-c-containing cytokine receptors. *Chemistry & Biology* **2011,** *18*, 314-323.

10. Thoma, G.; Drückes, P.; Zerwes, H.-G. Selective inhibitors of the janus kinase JAK3—are they effective? *Bioorganic & Medicinal Chemistry Letters* **2014,** *24* (19), 4617-4621.

11. Thorarensen, A.; Banker, M. E.; Fensome, A.; Telliez, J.-B.; Juba, B.; Vincent, F.; Czerwinski, R. M.; Casimiro-Garcia, A. ATP-mediated kinome selectivity: the missing link in

understanding the contribution of individual JAK kinase isoforms to cellular signaling. *ACS Chemical Biology* **2014,** *9* (7), 1552-1558.

12. Clark, J. D.; Flanagan, M. E.; Telliez, J.-B. Discovery and development of janus kinase (JAK) inhibitors for inflammatory diseases. *Journal of Medicinal Chemistry* **2014,** *57* (12), 5023-5038.

13. Dymock, B. W.; Yang, E. G.; Chu-Farseeva, Y.; Yao, L. Selective JAK inhibitors. *Future Medicinal Chemistry* **2014,** *6* (12), 1439-1471.

14. Welsch, K.; Holstein, J.; Laurence, A.; Ghoreschi, K. Targeting JAK/STAT signalling in inflammatory skin diseases with small molecule inhibitors. *European Journal of Immunology* **2017,** *47* (7), 1096-1107.

15. Flanagan, M. E.; Blumenkopf, T. A.; Brissette, W. H.; Brown, M. F.; Casavant, J. M.; Poa, C. S.; Doty, J. L.; Elliott, E. A.; Fisher, M. B.; Hines, M.; Kent, C.; Kudlacz, E. M.; Lillie, B. M.; Magnuson, K. S.; McCurdy, S. P.; Munchhof, M. J.; Perry, B. D.; Sawyer, P. S.; Strelevitz, T. J.; Subramanyam, C.; Sun, J.; Whipple, D. A.; Changelian, P. S. Discovery of CP-690'550: a potent and selective janus kinase (JAK) inhibitor for the treatment of autoimmune diseases and organ transplant rejection. *Journal of Medicinal Chemistry* **2010,** *53*, 8468-8484.

16. Thoma, G.; Nuninger, F.; Falchetto, R.; Hermes, E.; Tavares, G. A.; Vangrevelinghe, E.; Zerwes, H.-G. Identification of a potent janus Kinase 3 Inhibitor with high selectivity within the janus kinase family. *Journal of Medicinal Chemistry* **2011,** *54* (1), 284-288.

17. Chrencik, J. E.; Patny, A.; Leung, I. K.; Korniski, B.; Emmons, T. L.; Hall, T.; Weinberg, R. A.; Gormley, J. A.; Williams, J. M.; Day, J. E.; Hirsch, J. L.; Kiefer, J. R.; Leone, J. W.;

Fischer, H. D.; Sommers, C. D.; Huang, H.-C.; Jacobsen, E. J.; Tenbrink, R. E.; Tomasselli, A. G.; Benson, T. E. Structural and thermodynamic characterization of the TYK2 and JAK3 kinase domains in complex with CP-690550 and CMP-6. *Journal of Molecular Biology* **2010,** *400*, 413-433.

18. Chaikuad, A.; Koch, P.; Laufer, S.; Knapp, S. The cysteinome of protein kinases as a target in drug development. *Angewandte Chemie International Edition* **2018**, 57, 4372-4385.

19. Liu, Q.; Sabnis, Y.; Zhao, Z.; Zhang, T.; Buhrlage, Sara J.; Jones, Lyn H.; Gray, Nathanael S. Developing irreversible inhibitors of the protein kinase cysteinome. *Chemistry & Biology* **2013,** *20* (2), 146-159.

20. Elwood, F.; Witter, D.; Piesvaux, J.; Kraybill, B.; Bays, N.; Alpert, C.; Goldenblatt, P.; Qu, Y.; Ivanovska, I.; Lee, H.-H.; Chiu, C.-S.; Tang, H.; Scott, M. E.; Deshmukh, S.; Zielstorff, M.; Byford, A.; Chakravarty, K.; Dorosh, L.; Rivkin, A.; Klappenbach, J.; Pan, B.-S.; Kariv, I.; Dinsmore, C.; Slipetz, D.; Dandliker, P. Evaluation of JAK3 biology in autoimmune disease using a highly selective, irreversible JAK3 inhibitor. *Journal of Pharmacology and Experimental Therapeutics* **2017,** *361* (2), 229-244.

21. Forster, M.; Gehringer, M.; Laufer, S. A. Recent advances in JAK3 inhibition: isoform selectivity by covalent cysteine targeting. *Bioorganic & Medicinal Chemistry Letters* **2017,** *27* (18), 4229-4237.

22. Goedken, E. R.; Argiriadi, M. A.; Banach, D. L.; Fiamengo, B. A.; Foley, S. E.; Frank, K. E.; George, J. S.; Harris, C. M.; Hobson, A. D.; Ihle, D. C.; Marcotte, D.; Merta, P. J.; Michalak, M. E.; Murdock, S. E.; Tomlinson, M. J.; Voss, J. W. Tricyclic covalent inhibitors

selectively target JAK3 through an active site thiol. *Journal of Biological Chemistry* **2015,** *290* (8), 4573-4589.

23. London, N.; Miller, R. M.; Krishnan, S.; Uchida, K.; Irwin, J. J.; Eidam, O.; Gibold, L.; Cimermančič, P.; Bonnet, R.; Shoichet, B. K.; Taunton, J. Covalent docking of large libraries for the discovery of chemical probes. *Nature Chemical Biology* **2014,** *10* (12), 1066-1072.

24. Smith, G. A.; Uchida, K.; Weiss, A.; Taunton, J. Essential biphasic role for JAK3 catalytic activity in IL-2 receptor signaling. *Nature Chemical Biology* **2016,** *12* (5), 373-379.

25. Tan, L.; Akahane, K.; McNally, R.; Reyskens, K. M. S. E.; Ficarro, S. B.; Liu, S.; Herter-Sprie, G. S.; Koyama, S.; Pattison, M. J.; Labella, K.; Johannessen, L.; Akbay, E. A.; Wong, K.-K.; Frank, D. A.; Marto, J. A.; Look, T. A.; Arthur, J. S. C.; Eck, M. J.; Gray, N. S. Development of selective covalent janus kinase 3 inhibitors. *Journal of Medicinal Chemistry* **2015,** *58* (16), 6589-6606.

26. Thorarensen, A.; Dowty, M. E.; Banker, M. E.; Juba, B.; Jussif, J.; Lin, T.; Vincent, F.; Czerwinski, R. M.; Casimiro-Garcia, A.; Unwalla, R.; Trujillo, J. I.; Liang, S.; Balbo, P.; Che, Y.; Gilbert, A. M.; Brown, M. F.; Hayward, M.; Montgomery, J.; Leung, L.; Yang, X.; Soucy, S.; Hegen, M.; Coe, J.; Langille, J.; Vajdos, F.; Chrencik, J.; Telliez, J.-B. Design of a janus kinase 3 (JAK3) specific inhibitor 1-((2S,5R)-5-((7H-pyrrolo[2,3-d]pyrimidin-4-yl)amino)-2-methylpiperidin-1-yl)prop-2-en-1-one (PF-06651600) allowing for the interrogation of JAK3 signaling in humans. *Journal of Medicinal Chemistry* **2017,** *60* (5), 1971-1993

27. Forster, M.; Chaikuad, A.; Bauer, Silke M.; Holstein, J.; Robers, Matthew B.; Corona, Cesear R.; Gehringer, M.; Pfaffenrot, E.; Ghoreschi, K.; Knapp, S.; Laufer, S. A. Selective JAK3

inhibitors with a covalent reversible binding mode targeting a new induced fit binding pocket. *Cell Chemical Biology* **2016,** *23* (11), 1335-1340.

28. The structural genomics consortium: FM-381 a chemical probe for JAK3. http://www.thesgc.org/chemical-probes/FM-381 (accessed 05.01.2018).

29. The chemical probes portal: FM-381. http://www.chemicalprobes.org/fm-381 (accessed 05.01.2018).

30. Bauer, S. M.; Gehringer, M.; Laufer, S. A. A direct enzyme-linked immunosorbent assay (ELISA) for the quantitative evaluation of janus kinase 3 (JAK3) inhibitors. *Analytical Methods* **2014,** *6* (21), 8817-8822.

31. Serafimova, I. M.; Pufall, M. A.; Krishnan, S.; Duda, K.; Cohen, M. S.; Maglathlin, R. L.; McFarland, J. M.; Miller, R. M.; Frödin, M.; Taunton, J. Reversible targeting of noncatalytic cysteines with chemically tuned electrophiles. *Nature Chemical Biology* **2012,** *8* (5), 471-476.

32. Singh, J.; Petter, R. C.; Baillie, T. A.; Whitty, A. The resurgence of covalent drugs. *Nature Reviews Drug Discovery* **2011,** *10*, 307-317.

33. Robers, M. B.; Dart, M. L.; Woodroofe, C. C.; Zimprich, C. A.; Kirkland, T. A.; Machleidt, T.; Kupcho, K. R.; Levin, S.; Hartnett, J. R.; Zimmerman, K.; Niles, A. L.; Ohana, R. F.; Daniels, D. L.; Slater, M.; Wood, M. G.; Cong, M.; Cheng, Y.-Q.; Wood, K. V. Target engagement and drug residence time can be observed in living cells with BRET. *Nature Communications* **2015,** *6*.

34. Ghoreschi, K.; Jesson, M. I.; Li, X.; Lee, J. L.; Ghosh, S.; Alsup, J. W.; Warner, J. D.; Tanaka, M.; Steward-Tharp, S. M.; Gadina, M.; Thomas, C. J.; Minnerly, J. C.; Storer, C. E.;

LaBranche, T. P.; Radi, Z. A.; Dowty, M. E.; Head, R. D.; Meyer, D. M.; Kishore, N.; O'Shea, J. J. Modulation of innate and adaptive immune responses by tofacitinib (CP-690,550). *The Journal of Immunology* **2011,** *186* (7), 4234-4243.

35. Beaulieu, P. L.; Haché, B.; von Moos, E. A practical Oxone®-mediated, high-throughput, solution-phase synthesis of benzimidazoles from 1,2-phenylenediamines and aldehydes and its application to preparative scale synthesis. *Synthesis* **2003,** *2003* (11), 1683-1692.

36. Dess, D. B.; Martin, J. C. Readily accessible 12-I-5 oxidant for the conversion of primary and secondary alcohols to aldehydes and ketones. *The Journal of Organic Chemistry* **1983,** *48* (22), 4155-4156.

37. Hoover, J. M.; Stahl, S. S. Highly practical copper(I)/TEMPO catalyst system for chemoselective aerobic oxidation of primary alcohols. *Journal of the American Chemical Society* **2011,** *133* (42), 16901-16910.

38. Blanchette, M. A.; Choy, W.; Davis, J. T.; Essenfeld, A. P.; Masamune, S.; Roush, W. R.; Sakai, T. Horner-Wadsworth-Emmons reaction: use of lithium chloride and an amine for base-sensitive compounds. *Tetrahedron Letters* **1984,** *25* (21), 2183-2186.

39. Maetz, P.; Rodriguez, M. A simple preparation of N-protected chiral α-aminonitriles from N-protected α-amino acid amides. *Tetrahedron Letters* **1997,** *38* (24), 4221-4222.

40. Telliez, J.-B.; Dowty, M. E.; Wang, L.; Jussif, J.; Lin, T.; Li, L.; Moy, E.; Balbo, P.; Li, W.; Zhao, Y.; Crouse, K.; Dickinson, C.; Symanowicz, P.; Hegen, M.; Banker, M. E.; Vincent, F.; Unwalla, R.; Liang, S.; Gilbert, A. M.; Brown, M. F.; Hayward, M.; Montgomery, J.; Yang, X.; Bauman, J.; Trujillo, J. I.; Casimiro-Garcia, A.; Vajdos, F. F.; Leung, L.; Geoghegan, K. F.;

Quazi, A.; Xuan, D.; Jones, L.; Hett, E.; Wright, K.; Clark, J. D.; Thorarensen, A. Discovery of a JAK3-selective inhibitor: functional differentiation of JAK3-selective inhibition over pan-JAK or JAK1-selective inhibition. *ACS Chemical Biology* **2016,** *11* (12), 3442-3451.

41. Evans, P. Scaling and assessment of data quality. *Acta Crystallographica Section D* **2006,** *62* (1), 72-82.

42. Kabsch, W. Processing of X-ray snapshots from crystals in random orientations. *Acta Crystallographica Section D* **2014,** *70* (8), 2204-2216.

43. McCoy, A. J.; Grosse-Kunstleve, R. W.; Adams, P. D.; Winn, M. D.; Storoni, L. C.; Read, R. J. Phaser crystallographic software. *Journal of Applied Crystallography* **2007,** *40* (Pt 4), 658-674.

44. Emsley, P.; Lohkamp, B.; Scott, W. G.; Cowtan, K. Features and development of Coot. *Acta Crystallographica Section D* **2010,** *66* (4), 486-501.

45. Murshudov, G. N.; Skubak, P.; Lebedev, A. A.; Pannu, N. S.; Steiner, R. A.; Nicholls, R. A.; Winn, M. D.; Long, F.; Vagin, A. A. REFMAC5 for the refinement of macromolecular crystal structures. *Acta Crystallographica Section D* **2011,** *67* (4), 355-367.

46. Chen, V. B.; Arendall, W. B., III; Headd, J. J.; Keedy, D. A.; Immormino, R. M.; Kapral, G. J.; Murray, L. W.; Richardson, J. S.; Richardson, D. C. MolProbity: all-atom structure validation for macromolecular crystallography. *Acta Crystallographica Section D* **2010,** *66* (1), 12-21.

47. DeLano, W. L. *The PyMol Molecular Graphics System Version 0.99rc6*, 2002.

48. ZINC15 http://zinc15.docking.org/patterns/home/ (accessed 20.03.2018).

TABLE OF CONTENTS GRAPHIC

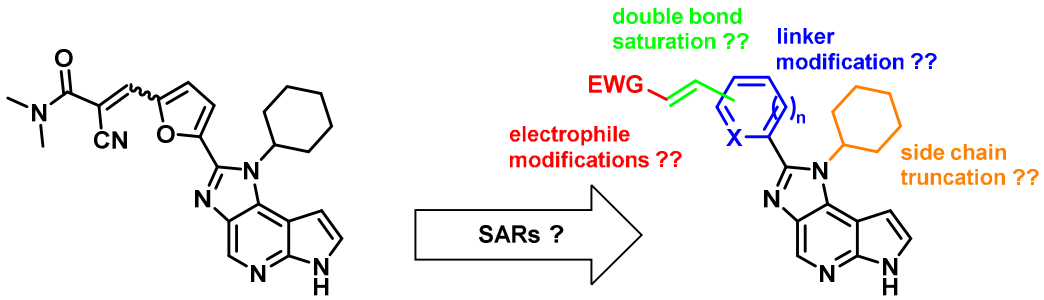

FM-381 **(23)**
JAK3 IC_{50} = 9 nM
high isoform selectivity